



Gambierdiscus polynesiensis from New Caledonia (South West Pacific Ocean): Morpho-molecular characterization, toxin profile and response to light intensity

Manoëlla Sibat^{a,*} , Tepoerau Mai^{b,c} , Nicolas Chomérat^d , Gwenael Bilien^d ,
Korian Lhaute^a , Philipp Hess^{a,e} , Véronique Séchet^e , Thierry Jauffrais^{b,*} 

^a Ifremer, ODE/PHYTOX-METALG, Rue de l'île d'Yeu, F-44300 Nantes, France

^b Ifremer, IRD, Univ Nouvelle-Calédonie, Univ La Réunion, CNRS, UMR 9220 ENTROPIE, BP 32078, 98800, Noumea, New Caledonia

^c Institut Louis Malardé (ILM), 98713 Papeete, Tahiti, French Polynesia

^d Ifremer, ODE/COAST/LERBO, Station Ifremer de Concarneau, Place de la Croix, Concarneau, F-29900, France

^e Ifremer, PHYTOX, Laboratoire PHYSALG, F-44300 Nantes, France

ARTICLE INFO

Keywords:

Gambierdiscus
Ciguatoxins
Harmful algal bloom
Phylogeny
Liquid chromatography-tandem mass spectrometry
PAM fluorometry
Chlorophyll a fluorescence

ABSTRACT

Gambierdiscus is known to produce neurotoxins associated with ciguatera poisoning (CP). In New Caledonia (NC), South West Pacific Ocean, there is currently a significant knowledge gap regarding CP and the microalgae linked to this foodborne illness. This study describes a new strain of *Gambierdiscus polynesiensis*, 19PV93, isolated from the west coast of NC. The strain was isolated and cultured for morpho-molecular characterization to determine its phylogenetic position. Toxic activity was assessed using a cell-based assay with neuroblastoma cells (CBA-N2a), and the toxin profile was characterized using liquid chromatography coupled with tandem mass spectrometry (LC-MS/MS) to evaluate potential risks to human health. Regarding the toxin profile, *G. polynesiensis* was characterized by the presence of gambierone, 44-methylgambierone (44-MeG), and an atypical ciguatoxin profile consisting solely of ciguatoxin-4A (CTX4A) and -4B (CTX4B). This finding confirms intraspecific variations in toxin profiles between strains from different geographic origins. In culture, *G. polynesiensis* demonstrated a preference for relatively low irradiances (50 to 100 $\mu\text{mol photons m}^{-2} \text{s}^{-1}$) compared to the higher light intensities often encountered in their natural environment. The impact of light on toxin concentrations was found to be inversely related to light intensity, with higher quotas observed at lower light levels. *Gambierdiscus* employed non-photochemical quenching as a photoprotective strategy to safeguard PSII from excessive light, particularly during both short-term and long-term exposure. However, this dissipation strategy alone appears insufficient, as photoinhibition was consistently observed, and the electron transfer rate and yield along the electron transfer chain rapidly declined with increasing light intensity.

1. Introduction

Microalgae are the primary food source of marine food webs and are essential for the ecosystem; however, some species are harmful and have the capacity to produce toxins causing severe poisoning to marine fauna and seafood consumers. In tropical coastal areas, Ciguatera Poisoning (CP) represents the main human intoxication of non-bacterial origin caused by the consumption of contaminated marine fish (Tester et al., 2013; Chinain et al., 2021) or seafood (Roué et al., 2016; Darius et al., 2017, 2018). Ciguatera poisoning is characterized by digestive,

neurological and cardiovascular disorders (Château-Degat et al., 2007; Friedman et al., 2017). This pathology is predominant in tropical island areas, and in all three major oceans: the Pacific Ocean, the Caribbean Basin and the Indian Ocean. French overseas areas particularly affected are French Polynesia, New Caledonia (NC), the French West Indies and Reunion Island (Chinain et al., 2010b; Clua et al., 2011; Hossen et al., 2013; Boisnoir et al., 2018).

At the end of the 1970s, ciguatoxins (CTXs) were identified as the main causative agents and subsequently associated with the genera *Gambierdiscus* and *Fukuyoa* (Adachi and Fukuyo, 1979; Bagnis et al.,

* Corresponding authors.

E-mail addresses: manoella.sibat@ifremer.fr (M. Sibat), tmai@ilm.pf (T. Mai), nicolas.chomerat@ifremer.fr (N. Chomérat), gwenael.bilien@ifremer.fr (G. Bilien), korian.lhaute@ifremer.fr (K. Lhaute), philipp.hess@ifremer.fr (P. Hess), veronique.sechet@ifremer.fr (V. Séchet), thierry.jauffrais@ifremer.fr (T. Jauffrais).

<https://doi.org/10.1016/j.hal.2025.102859>

Received 20 January 2025; Received in revised form 1 April 2025; Accepted 6 April 2025

Available online 9 April 2025

1568-9883/© 2025 The Author(s). Published by Elsevier B.V. This is an open access article under the CC BY license (<http://creativecommons.org/licenses/by/4.0/>).

1980; Gomez et al., 2015). CTXs are highly toxic lipophilic cyclic polyethers compounds that can be accumulated in the trophic chain and can be found in high concentrations in herbivorous reef fish, their carnivorous predators and other organisms in coral reef systems, including deep-sea fishes (Yogi et al., 2013; Roué et al., 2016; Darius et al., 2018, 2021; Oshiro et al., 2021; Oshiro, 2023). Other types of bioactive secondary metabolites, more hydrosoluble than CTXs, are known to be produced by the same genera including maitotoxins (MTXs) (Holmes et al., 1990; Murata and Yasumoto, 1995; Pisapia et al., 2020; Estevez et al., 2021; Murray et al., 2022), gambieric acids (GAs) (Nagai et al., 1993), gambieroxide (Watanabe et al., 2013), gambierol (Cuypers et al., 2008) and gambierones (Rodriguez et al., 2015; Murray et al., 2019, 2024; Yon et al., 2021b). Additionally, different analogs of CTXs are found in different regions (Lewis and Holmes, 1993; Vernoux and Lewis, 1997; Yasumoto, 2001; Hamilton et al., 2002; Diogene et al., 2017; Kryuchkov et al., 2020; Mudge et al., 2023), also highlighting the involvement of different species and/or strains of *Gambierdiscus* (Litaker et al., 2010; Longo et al., 2019) and the need to characterize *Gambierdiscus* spp. across all impacted regions.

The biodiversity and chemical diversity of these benthic dinoflagellates still need to be clarified/updated in some regions such as NC (Fukuyo, 1981). Furthermore, characterization of *Gambierdiscus* spp. toxicity related to toxin profiles is still a current challenge (Sibat et al., 2018; Estevez et al., 2020; Pisapia et al., 2020). The genus *Gambierdiscus* Adachi et Fukuyo (Adachi and Fukuyo, 1979) currently includes 19 accepted species (Chinain et al., 2020; Nguyen-Ngoc et al., 2023), and the closely related genus *Fukuyoa* (Gomez et al., 2015) includes four accepted species with two species i.e., *F. yasumotoi* and *F. ruetzleri*, formerly described as *Gambierdiscus* spp. (Holmes, 1998; Litaker et al., 2009). *Gambierdiscus* spp. are large and lenticular armoured cells with a fish-hook shaped apical pore (Hoppenrath et al., 2014). These benthic dinoflagellates are living as epiphytes on macroalgae (Adachi and Fukuyo, 1979; Bagnis et al., 1980).

In tropical coastal waters, *Gambierdiscus* species can form blooms influenced by various environmental factors such as light, temperature, and salinity. This study primarily focuses on the effect of light to understand how this key variable may affect the distribution, abundance, and relative toxicity of *Gambierdiscus*. Light is crucial for understanding the vertical distribution of *Gambierdiscus* spp. and their photo-physiological responses to light stress, which are not well-defined in tropical and subtropical shallow coral reef lagoons. These habitats are characterized by clear waters with a high penetration depth of the photosynthetically active radiation (PAR), reaching up to 2000 $\mu\text{mol m}^{-2} \text{s}^{-1}$ (Kirk, 1994; Pringault et al., 2005), and ultraviolet radiation, up to 2 W m^{-2} for UVB and 40 W m^{-2} for UVA (Torregiani and Lesser, 2007; Conan et al., 2008; Courtial et al., 2017).

Experimental data indicate that despite their presence in high light habitats, *Gambierdiscus* spp. are generally intolerant to high irradiance. Indeed, they have developed several behavioural strategies to cope with high irradiances, including cell aggregation, mucus production, active cell migration to shaded areas of host macrophytes as well as physiological responses such as the plasticity of cell size and chlorophyll content (for a review, (Chinain et al., 2021) and references therein). Species such as *G. australes*, *G. belizeanus*, *G. caribaeus*, *G. carolinianus*, *G. carpenteri*, *G. pacificus*, *G. ruetzleri*, *G. toxicus*, *G. scabrosus*, and others have optimal light levels between 50 to 200–300 $\mu\text{mol photons m}^{-2} \text{s}^{-1}$ (Bomber et al., 1988; Morton et al., 1992; Villareal and Morton, 2002; Kibler et al., 2012; Yoshimatsu et al., 2016; Vacarizas et al., 2018; Funaki et al., 2022). However, some species may tolerate higher light levels (>300 $\mu\text{mol photons m}^{-2} \text{s}^{-1}$) and still maintain growth, such as *G. belizeanus*, *G. carpenteri*, *F. ruetzleri*, (*ex-G. ruetzleri*), *G. australes*, *G. scabrosus*, *Gambierdiscus* ribotype 2 and *Gambierdiscus* sp. type 3 (Kibler et al., 2012; Yoshimatsu et al., 2016). For *G. polynesiensis*, the impact of light on growth and toxicity needs further clarification. Moreover, the photo-physiological plasticity of most *Gambierdiscus* species in coping with light fluctuations remains unclear (Villareal and Morton, 2002;

Leynse et al., 2017) and is unknown for *G. polynesiensis*. Light intensity in these habitats can fluctuate across both short-term (seconds to hours) and long-term (seasonal) timescales. These variations arise from predictable factors such as changes in day length, solar angle, and tidal cycles, as well as unpredictable influences like cloud cover or turbidity caused by terrestrial runoff, and sediment resuspension within lagoons (Jaufrais et al., 2022). In these conditions, *Gambierdiscus* species must optimize light use for photosynthesis while protecting their photosystems from excessive light.

In this study, we describe a new strain of *Gambierdiscus* isolated from Vata Bay, Nouméa, on the west coast of NC. The strain was isolated in September 2019, was associated with *Turbinaria ornata* and cultured for morpho-molecular characterization to ascertain its phylogenetic position. To assess potential risks to human health, its toxicity has been screened with the cell-based assay using neuroblastoma (CBA-N2a) and the characterization of its toxin profiles was determined using liquid chromatography coupled to tandem mass spectrometry (LC-MS/MS). Furthermore, the effects of different light levels were investigated for growth, toxin production and photosynthetic response using the chlorophyll-*a* fluorescence technique.

2. Material and methods

2.1. Study site, sampling and culture

New Caledonia is located in the Southwestern Pacific Ocean, approximately 1 500 km east of Australia. The region consists of several islands, including the main island called 'Grande Terre'. The island is surrounded by a 1 600 km long barrier reef, which marks the boundary of a vast 23 400 km^2 lagoon (Andrefouet et al., 2009). The strain was isolated in Vata Bay (Nouméa), on the west coast of Grande Terre (Fig. S1). In this study, one strain of *Gambierdiscus* (19PV93) was isolated in September 2019 from *Turbinaria ornata* on a degraded and anthropized reef, in a shallow water area (maximum depth ~2 m), situated in the northwestern part (22°18'15.3"S 166°26'09.8"E) of Vata Bay, in Nouméa.

Under a stereomicroscope, a single cell was isolated using an elongated Pasteur pipette and washed in several drops of filtered (0.2 μm) and autoclaved seawater before being transferred to multi-dishes containing filtered, autoclaved, and F/10 K enriched seawater (Holmes et al., 1991). The strain was placed in a thermo-controlled incubator at 28 °C and under 50 $\mu\text{mol photons m}^{-2} \text{s}^{-1}$ and after some divisions the strain was transferred to 150 mL Erlenmeyer flasks containing 50 mL F/10 K medium and maintained in our culture collection under similar conditions. The photoperiod was 14 h light /10 h dark.

For toxin analyses, *Gambierdiscus* was cultured in 1 000 mL Erlenmeyer flasks filled with 500 mL F/10 K culture medium at 28 °C and ~150 $\mu\text{mol photons m}^{-2} \text{s}^{-1}$, and gently aerated. When the cultures reached the stationary phase after three weeks of culture, the microalgae were centrifuged (4500 g, 5 min, 4 °C) and the algal cell pellet freeze-dried and stored at -80 °C until toxin analyses.

2.2. Microscopy observations

Live and Lugol-fixed cells were visualized using a Leica microscope (DM750, Leica Microsystems, Germany) and swimming pattern captured with an inverted microscope (Primovert, Zeiss, Germany) equipped with a DSLR camera (Nikon D500, Japan). Morphometric analysis was performed on these images using ImageJ software and Analyze Particles plugins (Schneider et al., 2012).

Gambierdiscus live cells in the growth phase were sampled from the culture and fixed in an acidic Lugol's solution (4 % final concentration) for SEM observation either at the Station of Marine Biology of Concarneau or in New Caledonia. In both cases, cells were filtered and rinsed several times with distilled water and subsequently, the fixed cells underwent a dehydration process in a series of ethanol baths (25 %, 50 %, 75 %, 95 %, 100 %).

70 %, 90 %, 95 %, and 100 % EtOH) for 20 min. In Concarneau, the cells were then critical point dried with a K850 CPD (EMS) using liquid CO₂, and then coated with gold using a 108Auto sputter coater (Cressington, UK). Observations were realized with a Sigma 300 field emission SEM (Carl Zeiss, Germany) at an acceleration of 1.5 kV and a working distance of 8 mm. In New Caledonia, cells were air-dried on a glass cover slide and afterward, an 8 nm platinum coating was applied to the samples using the LEICA EM ACE 600 and the samples were then imaged with an environmental SEM utilizing the secondary electron detector. (JSM-IT300 LV, 10 kV, 10 mm WD, JEOL, Japan).

2.3. Sequencing and phylogenetic analyses

Prior to amplification, DNA was extracted from culture aliquots (2 mL) of strain 19PV93 in exponential phase using the PCRBI0 Rapid Extract PCR kit (Eurobio) in accordance with the manufacturer's instructions. The amplification steps directly follow the extraction and two variable domains of the Large Subunit of the ribosome operon (LSU rDNA gene), namely D1-D3 and D8-D10 were targeted. The reactions used PCR Master Mix of the kit, with a final reaction volume of 25 µl and the primer pairs chosen were D1R-D3B (Scholin et al., 1994; Nunn et al., 1996) with an annealing temperature of 56 °C and FD8-RB (Chinain et al., 1999a, 1999b) (Ta 50 °C). Amplicons were visualized on a 1 % agarose gel. The PCR product was purified using the Illustra ExoProStar kit (Cytiva) then sequenced using the Sanger method to Microsynth Company (Lyon, France).

For phylogenetic analyses inferred from D1-D3 domains and D8-D10 domains of LSU rDNA, two datasets were prepared including sequences of *Gambierdiscus* and the related genus *Fukuyoa* retrieved from GenBank. The D1-D3 dataset included the sequence of strain 19PV93, 57 sequences of *Gambierdiscus* spp., 3 sequences of *Fukuyoa* spp. and 3 outgroup sequences and comprised 1158 characters (including gaps) in length. The D8-D10 dataset included the sequence of strain 19PV93 with 61 sequences of *Gambierdiscus* spp., 3 of *Fukuyoa* spp. and 3 outgroup sequences, and comprised 943 characters including gaps in length. Both datasets were aligned using MAFFT algorithm (Katoh and Standley, 2013) followed by refinement by eye. Phylogenetic reconstructions were performed using two methods: maximum likelihood (ML) using PHY-ML software v. 3.0 (Guindon et al., 2010) and bayesian inference (BI) using MrBayes software v.3.1.2 (Ronquist and Huelsenbeck, 2003). For ML analysis, a general-time-reversible (GTR) model was selected with gamma shape parameter and invariant sites, and a bootstrap analysis was carried out on 1 000 pseudo-replicates to assess the robustness of branches. Initial BI analyses were run with a GTR model (nst=6) with rates set to invgamma. The number of generations used in these analyses was 4 000 000, with sampling every 100th generations. The burnin values were set so that the first 4 000 trees were discarded and the posterior probabilities of each clade were calculated from the remaining 36 001 trees.

2.4. Toxin extraction

Lyophilized cell pellets (25 mg) were extracted thrice with 2 mL aqueous methanol 90 % using an ultrasonic bath (Elma, Singen, Germany) at 25 kHz in sweep mode during 15 min on ice. Once cells were disrupted, the supernatants were collected and combined after centrifugation at 3 500 g, 4 °C for 15 min. The extracts were evaporated to dryness under a gentle stream of nitrogen at 40 °C and re-suspended in MeOH 90 % (1 mL). The final extracts were filtered through a Nanosep MF 0.2 µm filter (Pall, Northborough, MA, USA) and stored at -20 °C before analysis.

2.5. Cell-based assay on *Neuroblasma* (CBA-N2a)

Neuroblastoma cell-based assay was used to determine the toxicity of the *Gambierdiscus* species, the test was performed using the protocol

previously described by Yon et al. (2021b). Briefly, cell exposure was performed by adding either 10 µL of Ouabain/Veratridin (O/V⁺) at 77 µM and 7.7 µM respectively to assess the presence of sodium channel activators or water (O/V) to assess the presence of non-specific toxic compounds in samples. Cell viability was assessed using the 3-(4,5-dimethylthiazol-2-yl)-2,5-diphenyl tetrazolium bromide (MTT) colorimetric assay and the cells were disrupted with dimethyl sulfoxide (DMSO) to measure the absorbance at 570 nm with a microplate reader (CLARIOstar PLUS, BMG Labtech, France). Sigmoidal dose-response curves were obtained with MARS software 4.00 (BMG Labtech), using a four-parameter logistic regression model to obtain the half-maximal effective concentration (EC₅₀), with no blank correction. Each sample was tested in three independent experiments. The CTX-like activity was estimated using a CTX3C reference material (Wako chemicals, Germany) ranging from 0.03 to 55.6 pg mL⁻¹. The final toxin content of the methanol extracts was expressed in fg CTX3C eq. cell⁻¹.

2.6. Liquid chromatography coupled to tandem mass spectrometry (LC-MS-MS)

To determine the toxin profile of the species of *Gambierdiscus*, two LC-MS/MS acquisition methods were used: a method for the P-CTX group based on the protocol by Sibat et al., 2018 (Sibat et al., 2018) and a second method for MTXs and Gambiertoxin group (which includes gambierones, gambieric acids and gambieroxide) based on Yon et al. (2021b) with slight modifications. Both experiments were performed using a UHPLC system (UFLC Nexera, SHIMADZU, Japan) coupled to a hybrid triple quadrupole-linear ion-trap API4000 QTRAP mass spectrometer (SCIEX, CA, USA) equipped with a TurboV® electrospray ionization source (ESI). The instrument control, data processing and analysis were conducted using Analyst software 1.7.2 (Sciex, CA, USA).

2.6.1. Standards and chemicals

LC-MS grade methanol, acetonitrile, formic acid (98 % purity) and ammonium formate were purchased from Sigma Aldrich GmbH (Steinheim, Germany). Water was deionized and purified at 18 MΩ cm⁻¹ through a Milli-Q integral 3 system (Millipore, France). CTX3C, CTX3B, CTX4A, CTX4B, M-seco-CTX3C, 2,3-dihydroxyCTX3C and 52-*epi*-54-deoxy CTX1B standards were provided by Institut Louis Malardé (ILM, Tahiti, French Polynesia). Due to the limited availability of standards, only a calibration solution of CTX3C was prepared in MeOH, with concentrations ranging from 5 to 2 000 ng mL⁻¹. A mix of P-CTX standards was also injected to obtain a toxin profile for verification of retention times. A standard of maitotoxin 1 (MTX1) was purchased from Wako (Wako chemical, Germany), gambierone and 44-methylgambierone (44-MeG) were purchased from Cifga (Cifga laboratory, Spain). To quantify the MTXs and Gambiertoxins, a calibration solution of MTX1, gambierone and 44-MeG was prepared in 50 % MeOH with concentrations ranging from 0.2 to 5.0 µg mL⁻¹ for MTX1 and 0.05 to 1.2 µg mL⁻¹ for gambierone and 44-MeG.

2.6.2. Method 1: Detection of P-CTX group

A linear gradient using water as eluent A and MeOH as eluent B, both eluents containing 2 mM ammonium formate and 50 mM formic acid, was run on a Zorbax Eclipse Plus C18 column, 50×2.1 mm, 1.8 µm, 95 Å (Agilent Technologies, CA, USA). The flow rate was set at 0.4 mL min⁻¹, the injection volume at 5 µL and the column temperature at 40 °C. The elution gradient ran from 78 % B to 88 % B over 10 min and was held during 4 min before returning to initial conditions and re-equilibration during 5 min. The optimized ESI⁺ parameters were set as follows: curtain gas at 25 psi, ion spray at 5 500 V, turbo gas temperature at 300 °C, gas 1 and 2 were set at 40 and 60 psi, respectively, and the entrance potential at 10 V.

The acquisition method was performed in positive ionization mode using scheduled Multiple Reaction Monitoring (MRM) algorithm. This algorithm optimizes dwell times and cycle time to provide a better peak

detection and improve reproducibility. A detection window of 120 s and a target scan time of 1.2 s were chosen for the P-CTXs group method. The m/z transition used were listed in **Table S1**. The limit of detection (LOD) and quantification (LOQ) for CTX3C were determined in [Sibat et al., 2018](#) at 2 and 6 ng mL⁻¹, respectively.

2.6.3. Method 2: Detection of MTX and gambiertoxins group

A linear gradient using water as eluent A and 95 % acetonitrile as eluent B, both eluents containing 2 mM ammonium formate and 50 mM formic acid, was run on a Kinetex C18 column, 50 × 2.1 mm, 2.6 μm, 100 Å (Phenomenex, CA, USA). The flow rate was of 0.4 mL min⁻¹, the injection volume was 5 μL and the column temperature set at 40 °C. The elution gradient was as follows: 10 % B to 95 % B from 0 to 10 min, hold at 95 % B for 2 min, decrease from 95 % to 10 % in 1 min and hold during 3 min to equilibrate. The optimized ESI parameters were set as follows: curtain gas at 25 psi, ion spray at -4 500 V, turbo gas temperature at 500 °C, gas 1 and 2 at 50 psi, declustering potential at -210 V and entrance potential at -10 V.

The acquisition method was performed in negative ionization mode using MRM scanning. The m/z transition used were listed in **Table S2**. The LOD and LOQ for MTX1, gambierone and 44-MeG, were calculated as three and 10 times the standard deviation, respectively, of the y-intercepts over the slope of the calibration curve ([Vial and Jardy, 1999](#); [Sanagi et al., 2009](#)) and listed in **Table S3**.

2.7. Response to light intensity

To evaluate the impact of photosynthetically active radiation (PAR) on the growth and toxin content of *G. polynesiensis* in batch culture, cells were inoculated with an aliquot from the linear growth phase of a stock culture. The cultures were grown in triplicate (150 mL of F/10 K culture medium) until they reached the stationary phase. The effects of light were assessed at intensities of 25, 50, 100, and 300 μmol photons m⁻² s⁻¹, measured with a spherical quantum sensor (LI-250 light meter, LI-COR), with cultures maintained at 28 °C under continuous light.

For toxin analysis, once the cultures reached the stationary phase, microalgal culture aliquots (10 mL) were centrifuged (4 500 g, 5 min, 4 °C). The algal pellet was then freeze-dried and stored at -80 °C. Cell growth was monitored daily through image analysis using ImageJ software ([Schneider et al., 2012](#)), combined with direct cell counting using a Nageotte counting cell under a Leica DM750 microscope (Leica Microsystems, Germany). To analyze growth kinetics under different light intensities, the data were fitted to a Gompertz model ([Eq. \(1\)](#)) ([Jauffrais et al., 2017](#)) using MATLAB software. This approach allowed for the estimation of key growth parameters, including the maximum growth rate (μ_{max} day⁻¹), the maximum cell concentration (α, expressed as ln(Ct/C0), where Ct and C0 represent cell density in cell mL⁻¹), and the latency phase duration (λ, in days, if present).

$$F(t) = \alpha \times \exp(-\exp(\mu_{\max} \times \exp(1) / \alpha \times (\lambda - t) + 1)) \quad (1)$$

All pulse-amplitude modulated (PAM) fluorescence measurements were conducted using a PAM fluorometer (AquaPen-P 110-P, Photon Systems Instruments, Drásov, Czech Republic) with a blue measuring light at 455 nm. The PAM probe was positioned on a stand holder just above the dark-acclimated (15 min) *Gambierdiscus* biofilm. To minimize the effects of growth-limiting factors, such as nitrogen depletion, on photophysiological parameters in batch culture, all measurements were taken during the linear growth phase across all conditions.

Photosynthetic functionality was assessed by measuring PSII maximum quantum efficiency (Fv/Fm, used as a proxy of the efficiency of the PSII light utilization for photochemical conversion) and by using parameters from rapid light curves (RLC, e.g., ([Perkins et al., 2006](#)), used as a proxy of photosynthesis vs irradiance curves) during growth phases (**Table S4**).

Rapid light curves were constructed using seven incremental light steps (10, 20, 50, 100, 300, 500, and 1 000 μmol photons m⁻² s⁻¹), each

lasting 60 s ([Coulombier et al., 2021](#)). The following parameters were extracted from the RLCs: alpha (α), the initial slope of the RLC at limiting irradiance represents the ability to use low light intensities; rETR_{max}, the maximum relative electron transport rate represents the photosynthetic activity; E_k, the light saturation coefficient represents the ability to use high light intensities; E_{opt}, the optimum light and beta (β) the photo inhibition coefficient ([Platt et al., 1980](#)).

These curves were also used to calculate non-photochemical quenching (NPQ)-induced response curves to light according [Serodio et al. \(2005\)](#).

Additionally, fast fluorescence transient kinetics (OJIP) were measured, to follow the physiological state of the microalgae, by exposing *Gambierdiscus* to a saturating flash of 2 100 μmol photons m⁻² s⁻¹ for 2 s, following the manufacturer's specifications. OJIP measures the polyphasic fluorescence transients during exposure to saturating light intensity, characterized by a rapid rise from the initial fluorescence intensity F₀ (designated as O) to a maximum intensity F_m (designated as P), via two intermediate inflection injection points, J and I, followed by a subsequent decline ([Strasser and Strasser, 1995](#); [Strasser et al., 2000](#); [Meriot et al., 2024](#)). The slope of the corresponding OJIP transient represents the physiological state of the microalgae and provided insights into photo-physiological parameters (**Table S5**). These include the specific energy flux per reaction center (RC) for energy absorption (ABS/RC), trapped energy flux (TR0/RC), electron transport flux (ET0/RC), dissipated energy flux (DIO/RC) and the Performance Index for energy conservation from photons absorbed by PSII until the reduction of intersystem electron acceptors by RC (PI ABS).

2.8. Statistical analysis

Data are expressed as mean ± standard deviation (SD). Depending on the data, statistical analyses consisted either in one-way analysis of variance (ANOVA), or in a Kruskal–Wallis test, followed, when necessary, by a Fisher's least significant difference procedure or Dunn tests. Differences were considered significant at p < 0.05. Before each ANOVA analysis or Kruskal–Wallis test, normality and equality of variance were tested to decide which test was going to be used. Statistical analyses were carried out using Statgraphics Centurion XV.I (StatPoint Technologies, Inc.).

3. Results

The New-Caledonian strain described in the present study is, to our knowledge, the first strain of *Gambierdiscus polynesiensis* to be isolated outside Polynesia (as opposed to Melanesia and Micronesia regions). Its characterization was conducted using a morpho-molecular approach combined with toxin analysis and assessment of its toxicity towards neuroblastoma. We observed many similarities and some differences in the thecal morphology and toxin profile of *G. polynesiensis* ([Chinain et al., 1999a](#); [Yon et al., 2021a](#)), compared to those of the strain isolated in the present study (19PV93).

3.1. Morpho-molecular characterization

Cells of strain 19PV93 had a dorso-ventral (DV) length (depth) comprised between 42.3 and 76.9 μm (DV = 61.6 ± 6.3 μm, n = 159), and cell width (W) ranged from 39.7 to 80.8 μm (W = 61.4 ± 6.6 μm, n = 159). The DV/W ratio was between 1.3 and 0.8 (DV/W = 1.01 ± 0.09, n = 159). The result of the morphometric analysis was highly dependent of the size of the *Gambierdiscus* (small vs large cells) cell (**Fig. 1**). In apical and antapical views, cells were round-shaped to slightly laterally compressed (**Fig. 1**; **Fig. 2A–D**). Cells were lenticular, biconvex, with a cingulum narrow in lateral view (**Fig. 2A–D**).

The plate formula was interpreted as Po, 4', 6", 6C, 6?S, 5"', 2'''' but not all small sulcal platelets could be clearly observed. The pore plate (Po) was central and slightly displaced ventrally on the epitheca (**Figs**

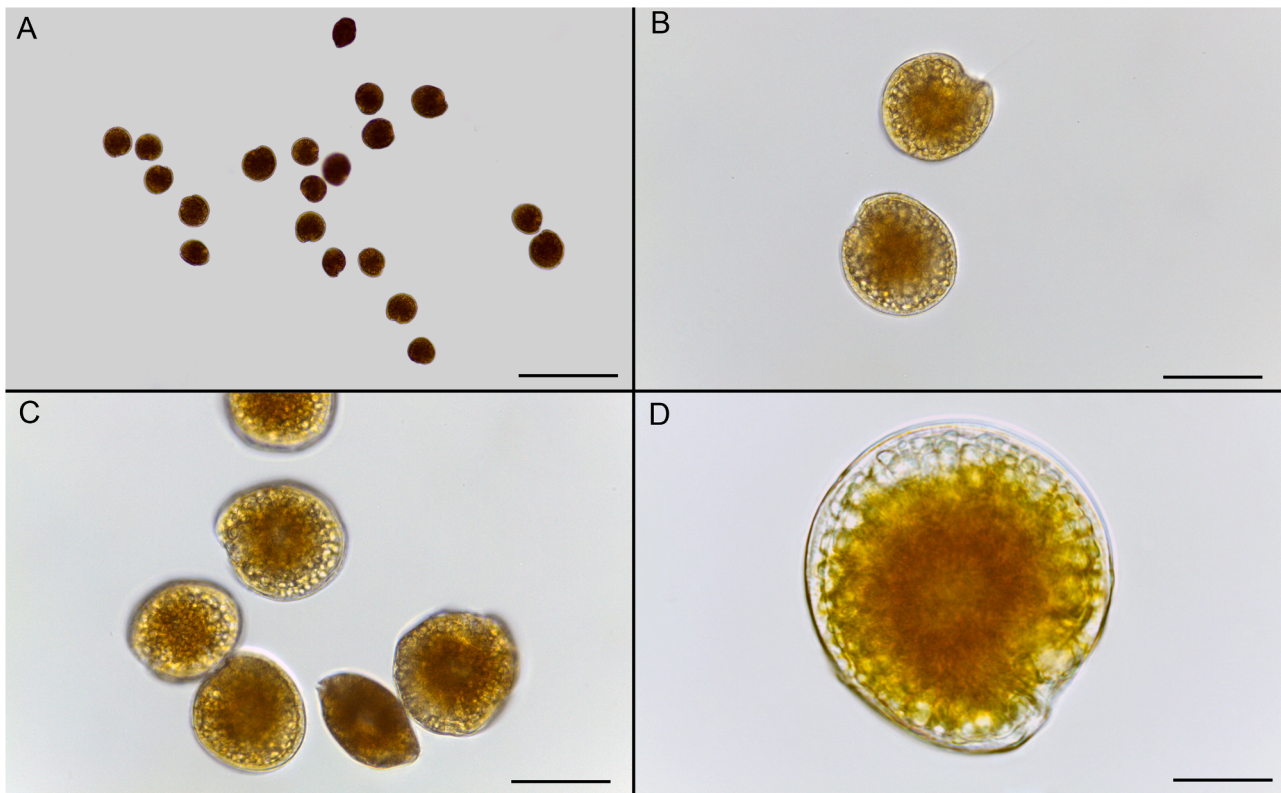


Fig. 1. Light micrographs of *Gambierdiscus polynesiensis* cells from strain 19PV93 from Vata Bay (Nouméa). (A) low magnification; (B, C, D) high magnification. Scale bars: (A) 200 μm , (B, C) 50 μm , (D) 20 μm .

2A, D). It was large and triangular-shaped, with a fish-hook shaped apical pore surrounded by a row of pores evenly distributed (Fig. 2F). The number of pores of the Po plate was also slightly variable, 36.3 ± 2.5 between cells ($n = 8$, Fig. S2). Among characteristic plates, plate 2' was the largest of the epitheca and hatchet-shaped (i.e., suture 1''/2' shorter than 2'/3''), but this was quite variable in the culture and the asymmetry was more or less pronounced (Figs 1A, D). Furthermore, a 'fold' of the 1'' plate was observed on its side in contact with the narrow and elongated plate 1' (Fig. 2C, 2E). On the hypotheca, the most conspicuous plate was the broad and pentagonal plate 2''', wedged between plates Sp, 1''', 2'', 3''' and 4''' (Fig 2B). It occupied the major part of the hypotheca (> 60 % of the surface).

The thecal surface of the cell was smooth and covered with small and round pores evenly distributed on each thecal plate (Fig. 2G).

From a phylogenetic point of view, the ML trees inferred from both D1-D3 domains and D8-D10 domains of LSU rDNA (Fig. 3 and Fig. 4) were congruent and showed that the sequences of *Gambierdiscus* 19PV93 isolated in New Caledonia clustered in a well-supported clade comprising strains RG92-1/2, Gpoly, TB-92-2/3/4, CAWD212, CG14/15 all identified as *G. polynesiensis*. Sequences of strain 19PV93 were not strictly identical with those already available for other strains. For instance, the D1-D3 sequence of 19PV93 showed 7 to 10 base differences with sequences of strains RG12-1, TB92-2, TB92-3, TB92-4, CG15, Gpoly and CAWD212 while it had 2 to 14 other base differences in separate loci with strains TB92-2, RG92-2, CG15 and CG14.

3.2. Toxicity assessment by CBA-N2a and toxin profile by LC-MS/MS

The evaluation of CTX-like activity was conducted by CBA-N2a on the methanol extract of *G. polynesiensis* after three weeks of culture (stationary phase). The sigmoidal dose-response curve was obtained in O/V⁺ conditions (Fig. 5), the EC50 (cell mL⁻¹) was equal to 145.0 ± 5.5 which can be converted to a toxicity of 79.5 ± 7.2 fg CTX3C eq cell⁻¹

(Table 1).

The methanol extracts from *G. polynesiensis* harvested at the stationary phase were analyzed by LC-MS/MS using two screening approaches based on their ionization preference. In ESI⁺ mode, the toxin profile of *G. polynesiensis*, 19PV93, was characterized by the presence of gambierone at 5.81 min and 44-MeG at 6.05 min (Fig. 6, b, d). With reference materials for gambierone and 44-MeG available, the quantitative amounts were 1.4 and 0.92 pg cell⁻¹, respectively (Table 1). Neither gambieric acids, gambieroxide nor maitotoxins were detected in the strain 19PV93.

The CTX profile of *G. polynesiensis*, determined in positive MRM mode (Fig 6b, c), consisted solely of CTX4A and CTX4B, found at 13.4 and 16.9 fg CTX3C eq cell⁻¹, respectively (Table 1).

3.3. Photophysiological characterization of *G. polynesiensis*

3.3.1. Growth of *G. polynesiensis*

Light intensity significantly influenced the growth of *G. polynesiensis*, with three out of the four growth parameters studied showing statistical differences (Table 2). The maximum growth rates (μ_{max} , $p < 0.005$, Table 2; Fig. 7) were reduced under high light (HL) conditions (300 $\mu\text{mol photons m}^{-2} \text{s}^{-1}$, $\mu_{\text{max}} < 0.1 \text{ day}^{-1}$), while medium light (ML) conditions (100 $\mu\text{mol photons m}^{-2} \text{s}^{-1}$) induced the highest maximum growth rates ($\mu_{\text{max}} > 0.4 \text{ day}^{-1}$). In contrast, the lowest light (LL) intensities (25 and 50 $\mu\text{mol photons m}^{-2} \text{s}^{-1}$) resulted in intermediate growth rates ($\mu_{\text{max}} = 0.25 \text{ day}^{-1}$). A similar trend was observed for the number of cell divisions ($p < 0.005$) and the maximum cell concentration ($p < 0.005$), except for C_{max} at 25 $\mu\text{mol photons m}^{-2} \text{s}^{-1}$, which reached values comparable to those at 100 $\mu\text{mol photons m}^{-2} \text{s}^{-1}$. However, no significant differences were observed regarding the latency time ($p = 0.91$), which remained consistent across all conditions.

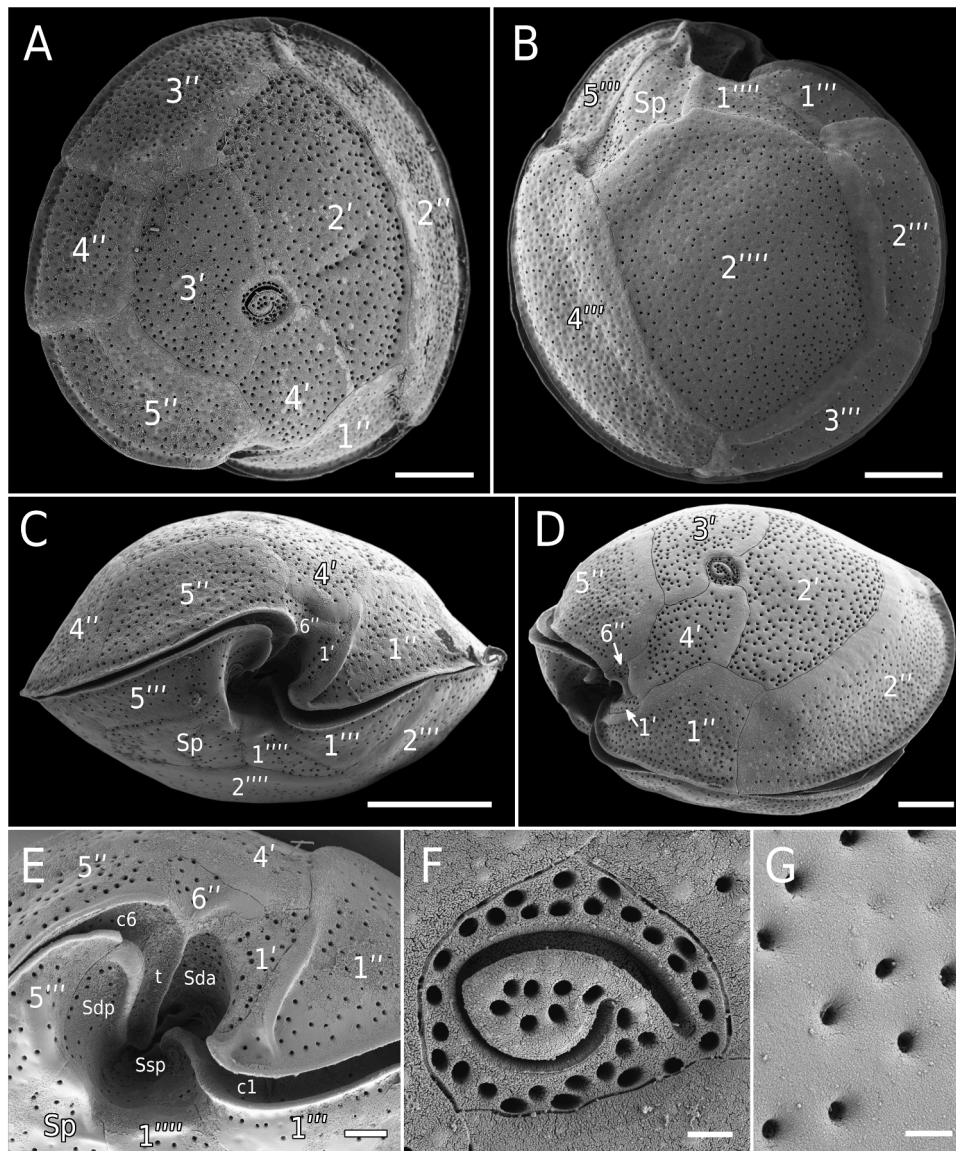


Fig. 2. Scanning electron micrographs of the thecal plates of *Gambierdiscus polynesiensis* (19PV93) from Vata Bay (Nouméa). A. Apical view of cells showing the smooth surface and the epithelial plates of the cell, the shape is round with an apical pore plate (Po) oriented ventrally; B. Antapical views showing the hypothecal plates of cells with the sulcal area visible. C. Ventral view showing the antero-posterior compression and lenticular shape. D. Left-oblique lateral view. D. Left-oblique lateral view. E. Detail of the sulcal area. F. Detail of the ellipsoid Po plates with a fish-hook shaped apical pore surrounded by rows of pores evenly distributed. G. Detail of the smooth thecal surface scattered with pores. Scale bars: A-D: 10 μm , E-G: 1 μm . Scale bars: A and B 10 μm , C 1 μm and D 5 μm .

3.3.2. Toxin concentrations

The impact of light is also evident on CTX and gambierone concentrations (Fig. 8 and Table 2). The cellular CTX and gambierone concentrations were found to be inversely related to light intensity, with higher concentrations observed under LL conditions (25 $\mu\text{mol photons m}^{-2} \text{s}^{-1}$) showing an overall toxicity of $1.96 \pm 0.44 \text{ pg cell}^{-1}$ for CTX and $85.4 \pm 17.5 \text{ pg cell}^{-1}$ for the gambierone toxins. In contrast, under HL conditions (300 $\mu\text{mol photons m}^{-2} \text{s}^{-1}$), no CTXs were detected and the total gambierone toxins content was found at $9.9 \pm 5.3 \text{ pg cell}^{-1}$.

3.3.3. Maximum quantum efficiency of PSII

Fv/Fm was used as an indicator of the quantum efficiency of PSII for photochemical conversion. Overall, Fv/Fm values were relatively low across all tested conditions (ranging from 0.16 ± 0.03 to 0.63 ± 0.02). However, significant differences were observed between the conditions ($p < 0.005$, Table 2, Fig. 9). Notably, Fv/Fm was significantly higher in cells grown under 50 $\mu\text{mol photons m}^{-2} \text{s}^{-1}$ ($Fv/Fm = 0.63 \pm 0.02$) compared to those grown under other conditions, where values ranged

from 0.16 ± 0.03 to 0.45 ± 0.03 .

3.3.4. RLC parameters

PAM fluorescence RLC were built using a saturating flash pulse at increasing actinic light intensity. RLC parameters (alpha, rETRmax, Ek, beta) and NPQ induced by the RLCs showed different patterns and significant differences between light conditions (Fig. 9 and Table 2). Photoinhibition (beta) was observed, highlighting the light sensitivity of this species under all conditions tested. Regarding the maximum relative electron transport rate, rETRmax, the highest values were observed in *G. polynesiensis* exposed to LL (25 $\mu\text{mol photons m}^{-2} \text{s}^{-1}$), with a gradual and significant ($p < 0.005$) decrease from 25 (54 ± 4) to 100 $\mu\text{mol photons m}^{-2} \text{s}^{-1}$ and similar values between 100 and 300 $\mu\text{mol photons m}^{-2} \text{s}^{-1}$ (29 ± 4). Often used as an indicator of LL acclimation, the highest light-utilization coefficient (α) was observed at 50 $\mu\text{mol photons m}^{-2} \text{s}^{-1}$, while the lowest was observed at 100 $\mu\text{mol photons m}^{-2} \text{s}^{-1}$, with intermediate and comparable values at 25 and 300 $\mu\text{mol photons m}^{-2} \text{s}^{-1}$ (Fig. 9 and Table 2). The light-saturating coefficient Ek, often used at a

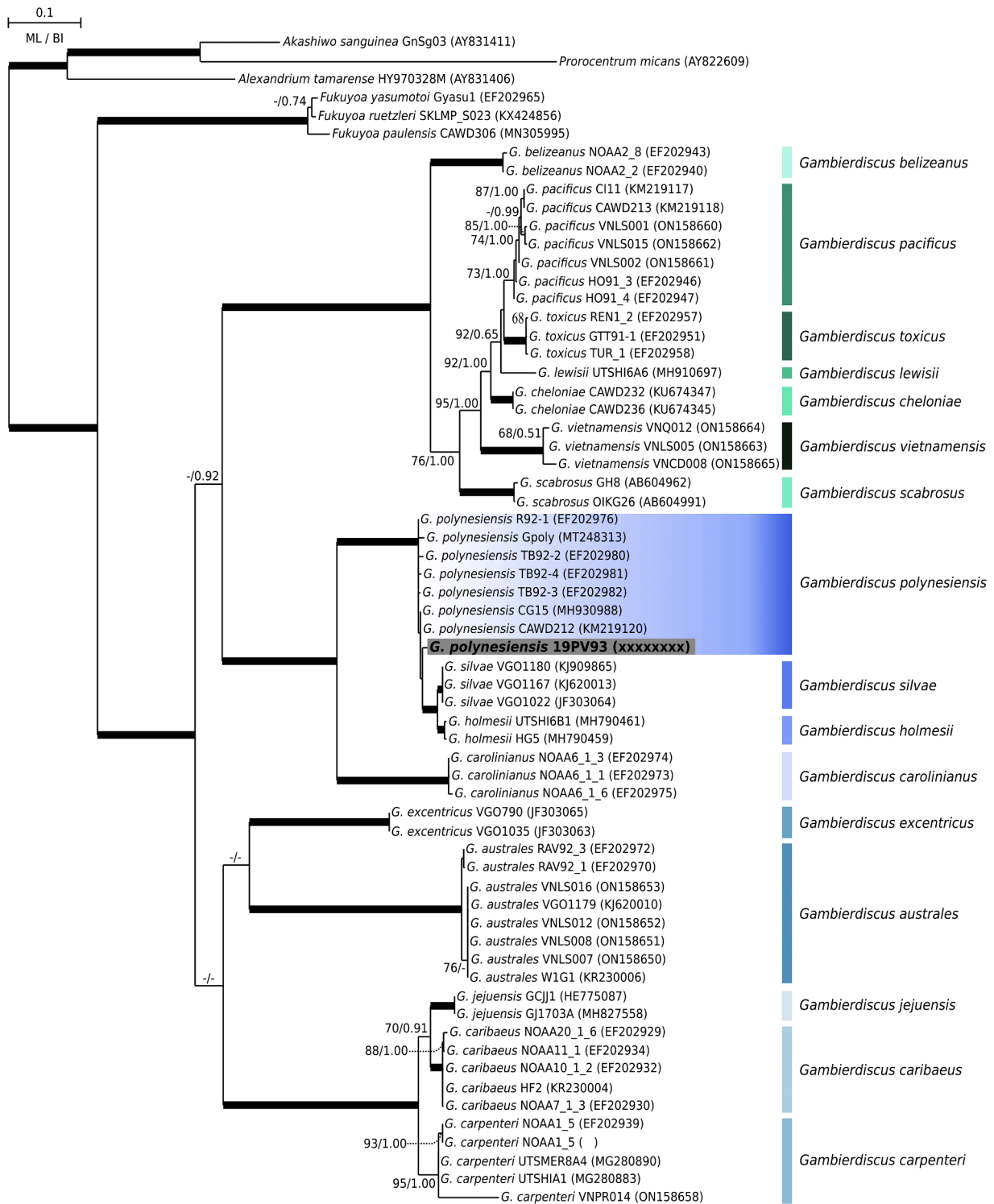


Fig. 3. Maximum Likelihood phylogenetic tree inferred from LSU rDNA D1–D3 sequences of various *Gambierdiscus*. Sequences from the present study are in bold face on a grey background. *Prorocentrum micans*, *Alexandrium tamarense* and *Akashiwo sanguinea* are used as outgroups. Vertical bars show distinct *Gambierdiscus* species. Numbers at nodes represent bootstrap support values from Maximum Likelihood (ML) and posterior probabilities from Bayesian Inference (BI). Bootstraps values below 65 and posterior probabilities below 0.70 are indicated with ‘-’.

proxy of the ability to use high light intensities, was high at LL ($284 \pm 36 \mu\text{mol photons m}^{-2} \text{s}^{-1}$) and slowly decreasing toward HL intensities ($148 \pm 6 \mu\text{mol photons m}^{-2} \text{s}^{-1}$, Table 2). The same pattern was observed for Eopt (the irradiance at which rETR is maximal). The kinetic of the NPQ response curves also differed between conditions, with the presence of a remaining NPQ at the beginning of the curves in the HL conditions;

whereas, at LL the NPQ remaining was close to zero. Similarly, values at the end of the RLCs differed, with low values observed at LL (<0.3), increasing quickly to similar values (0.47–0.60) from 50 to 300 $\mu\text{mol photons m}^{-2} \text{s}^{-1}$.

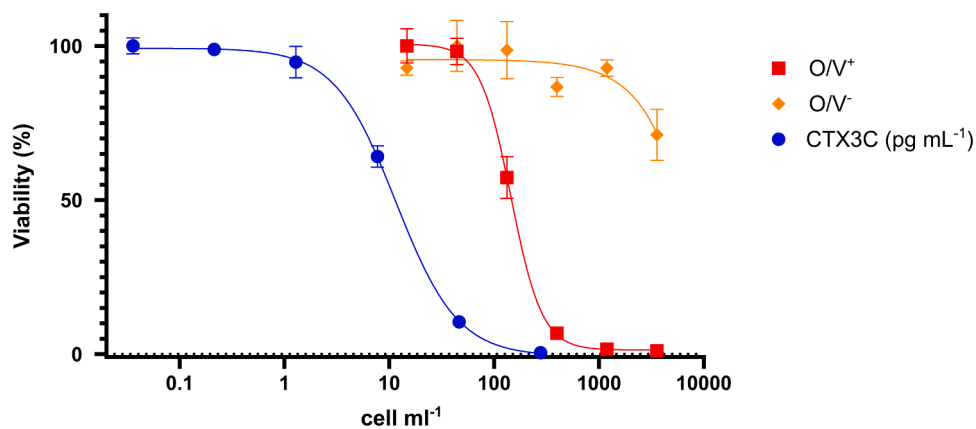


Fig. 5. Neuro2a cell-based assay dose response curves of *Gambierdiscus polynesiensis* in O/V⁺ condition (77 / 7.7 μM) (red) without O/V⁻ (orange) and a solution of CTX3C standard (Wako chemicals, Germany) (blue). Data represent the mean of three independent experiments with the standard deviation (± SD).

Table 1

Toxin concentrations (LC-MS/MS, API4000Qtrap) on an early stationary phase culture of *Gambierdiscus polynesiensis* (19PV93) and results of the cellular bioassay on neuroblastoma cells (CBA-N2a).

LC-MS/MS					CBA-N2a		
pg cell ⁻¹		fg CTX3C eq cell ⁻¹			cell mL ⁻¹	pg mL ⁻¹	fg CTX3C eq cell ⁻¹
Gambierone	44-MeG	CTX4A	CTX4B	Total	EC50 ± SD	EC50 ± SD	CTX content
1.4	0.92	13.4	16.9	30.3	145.0 ± 5.5	11.6 ± 0.7	79.5 ± 7.2

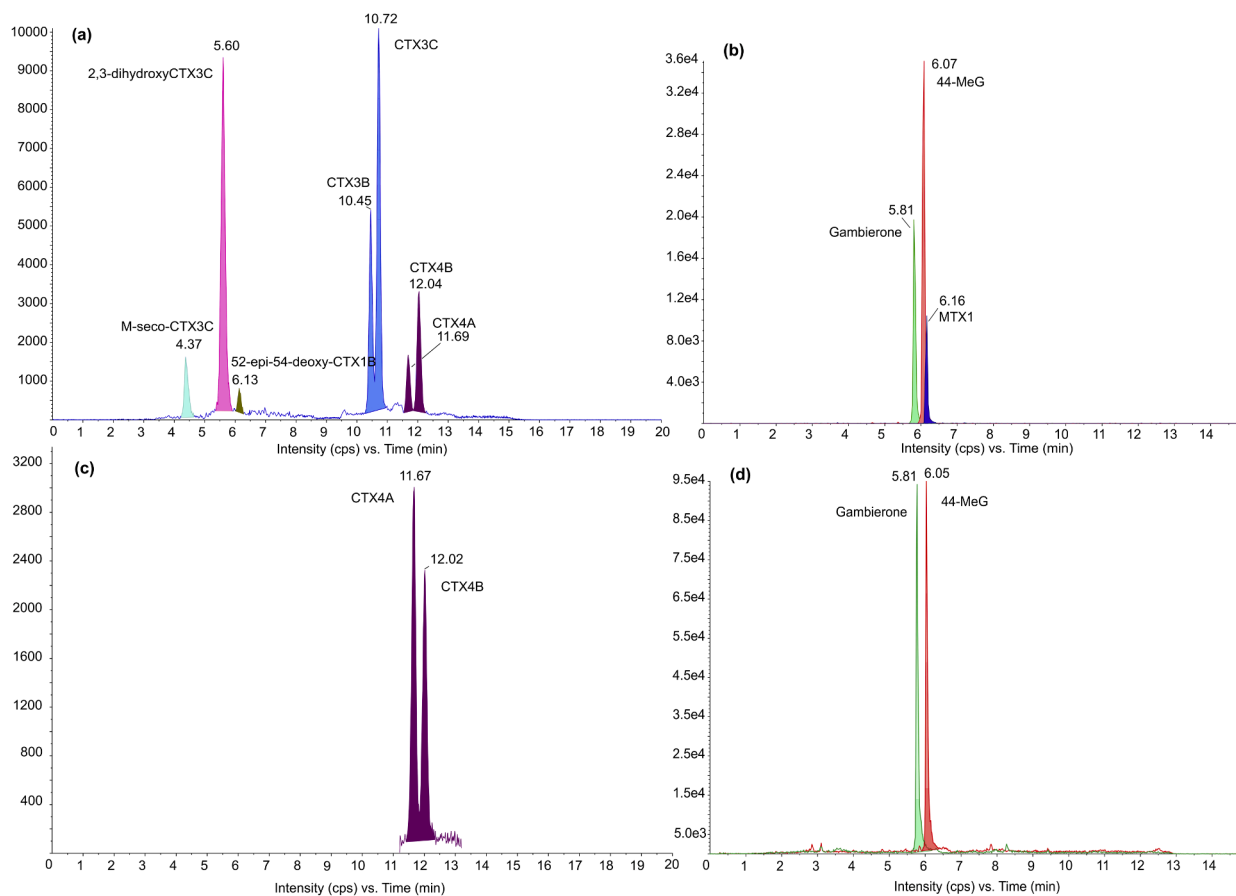


Fig. 6. LC-MS/MS chromatogram of (a) Mix of CTX standards (ILM, French Polynesia); (b) Mix of MTX1 (Wako chemicals, Germany), Gambierone and 44-MeG standards (Cifga, Spain); (c) and (d) *Gambierdiscus polynesiensis* sample; using the most intense MRM transition for each toxin.

Table 2

General growth and photophysiological characteristics as well as toxin concentrations of *Gambierdiscus polynesiensis* grown under different irradiance (PAR in $\mu\text{mol photons m}^{-2} \text{ s}^{-1}$). Values with the same letter (a, b or c) are not significantly different (Fisher, $p > 0.05$, mean \pm SD, $n = 3$).

	PAR 25	PAR 50	PAR 100	PAR 300	F-ratio	P-value
<i>Growth</i>						
μmax (day^{-1})	0.24 \pm 0.14b	0.26 \pm 0.06b	0.44 \pm 0.02c	0.06 \pm 0.01a	57.85	<0.005
Latency time, λ (day)	0.58 \pm 0.51	1.12 \pm 1.36	1.03 \pm 0.63	0.81 \pm 1.10	–	0.91
nbr div	3.68 \pm 0.13b	3.57 \pm 0.16b	4.8 \pm 0.56c	1.17 \pm 0.17a	73.28	<0.005
Cmax (cell mL^{-1})	2505 \pm 213c	1269 \pm 54b	2119 \pm 675c	410 \pm 44a	20.63	<0.005
<i>Toxin concentrations</i>						
CTX4A (pg cell $^{-1}$)	1.10 \pm 0.28b	0.30 \pm 0.10a	0.18 \pm 0.06a	<LOD*		0.035
CTX4B (pg cell $^{-1}$)	0.86 \pm 0.16b	0.17 \pm 0.07a	0.11 \pm 0.08a	<LOD		0.029
Gambierone (pg cell $^{-1}$)	66.8 \pm 9.4c	24.4 \pm 13.1b	6.6 \pm 0.08a	5.6 \pm 4.4a		0.032
44-MeG (pg cell $^{-1}$)	18.6 \pm 8.1b	14.9 \pm 7.7b	5.0 \pm 1.0a	4.3 \pm 0.9a		0.042
<i>Photophysiological parameters</i>						
Fv/Fm	0.45 \pm 0.03b	0.63 \pm 0.02c	0.30 \pm 0.02b	0.16 \pm 0.03a	23.36	<0.005
<i>RLCs</i>						
rETRmax	54 \pm 4b	43 \pm 3b	29 \pm 4a	29 \pm 1a	17.76	<0.05
Alpha, α	0.19 \pm 0.02 ab	0.24 \pm 0.02c	0.15 \pm 0.01b	0.20 \pm 0.01a	9.54	<0.05
Beta, β	0.98 \pm 0.02	0.54 \pm 0.13	0.67 \pm 0.34	0.68 \pm 0.32	–	0.94
Ek ($\mu\text{mol photon m}^{-2} \text{ s}^{-1}$)	284 \pm 36c	177 \pm 4ab	188 \pm 17b	148 \pm 6a	–	<0.05
Eopt ($\mu\text{mol photon m}^{-2} \text{ s}^{-1}$)	773 \pm 1d	490 \pm 12b	534 \pm 23c	422 \pm 7a	127.8	<0.005
NPQinduced	0.30 \pm 0.01a	0.47 \pm 0.03ab	0.60 \pm 0.12b	0.53 \pm 0.04b	3.62	0.06
<i>OJIP test-Specific fluxes</i>						
ABS/RC	3.41 \pm 0.29b	2.68 \pm 0.25a	4.78 \pm 0.80b	14.93 \pm 7.55c	–	<0.05
TR ₀ /RC	1.54 \pm 0.08	1.60 \pm 0.10	2.44 \pm 0.16	2.66 \pm 1.03	–	0.08
ET ₀ /RC	0.98 \pm 0.02	0.94 \pm 0.03	1.06 \pm 0.07	0.87 \pm 0.64	0.08	0.97
DI ₀ /RC	1.87 \pm 0.24a	1.11 \pm 0.15a	2.34 \pm 0.64a	12.27 \pm 6.54b	–	<0.05
<i>OJIP test-Quantum efficiency</i>						
M0	0.56 \pm 0.06	0.62 \pm 0.13	1.39 \pm 0.12	1.79 \pm 0.39	–	0.07
ϕP0	0.45 \pm 0.03b	0.59 \pm 0.02d	0.51 \pm 0.02c	0.19 \pm 0.03	167.33	<0.005
ψ0	0.63 \pm 0.02c	0.60 \pm 0.05ab	0.43 \pm 0.05bc	0.30 \pm 0.11a	14.39	<0.005
ϕE0	0.29 \pm 0.02b	0.35 \pm 0.04c	0.22 \pm 0.03b	0.05 \pm 0.02a	65.44	<0.005

Table 2 (continued)

	PAR 25	PAR 50	PAR 100	PAR 300	F-ratio	P-value
ϕD0	0.55 \pm 0.03b	0.41 \pm 0.02a	0.49 \pm 0.02b	0.82 \pm 0.03c	167.33	<0.005
<i>Performance index</i>						
Pi_Abs	0.43 \pm 0.08b	0.84 \pm 0.30c	0.17 \pm 0.003ab	0.007 \pm 0.003a	11.32	<0.05

* LOD: limit of detection (Table S3).

other conditions. The rate of reaction center closure (M0) increases with light intensity, showing the lowest values at LL and the highest values at HL but without showing significant differences. Regarding quantum efficiency parameters, the best yield of energy transfer (ϕP0 , ψ0 , ϕE0) and the lowest yield of dissipation (ϕD0) occurred at 50 $\mu\text{mol photons m}^{-2} \text{ s}^{-1}$. This is highlighted by PiABS, a performance index reflecting the probability that a trapped electron in the reaction center proceeds beyond the plastoquinone pool (PQ) in the electron transport chain. Indeed, PiABS is significantly higher at 50 $\mu\text{mol photons m}^{-2} \text{ s}^{-1}$, indicating an optimum photosynthetic performance at this irradiance. The PiABS values rapidly decrease at both lower and higher PAR levels.

4. Discussion

4.1. Morpho-molecular and toxin profile characterization

Both morphological observations and phylogenetic data are congruent to identify the strain 19PV93 as *Gambierdiscus polynesiensis*. Although we observed some variations in size in cultured cells, the overall morphology is in complete agreement with the original description of *G. polynesiensis* by (Chinain et al., 1999a). The surface was smooth and covered with small and round pores evenly distributed on each thecal plate. The triangular shape of the Po plate was remarkably similar in cells from 19PV93 and the original description (36.3 ± 2.5 vs 38 ± 3.4 for Tahitian strain TB-92), and the diagnostic plates 2' and 2''' (interpreted as 1p in some works) are typical of *G. polynesiensis* (Litaker et al., 2009). The presence of the thickened right edge of plate 1' in contact with 1', interpreted as a 'fold' by Litaker et al. (2009) is also a typical feature of *G. polynesiensis*. However, dorso-ventral (DV) cell length of 19PV93 was smaller ($DV = 77\text{--}42 \mu\text{m}$) than in specimens from the type locality ($DV = 85\text{--}68 \mu\text{m}$ long), whereas the width was much more variable ($W = 80.8\text{--}39.7 \mu\text{m}$) than the type locality with $75\text{--}64 \mu\text{m}$ wide (Chinain et al., 1999a). Nevertheless, the mean DV/W ratio were similar as cells were rounded ($D/W = 1$) in both strains. Moreover, phylogenetic analyses reveal that 19PV93 belongs to the *G. polynesiensis* clade and confirm unambiguously the identification (Chinain et al., 1999a).

Regarding the toxin profile, the strain 19PV93 was characterized by the presence of gambierone, 44-methylgambierone and an atypical CTX profile consisting solely of CTX4A and CTX4B. P-CTXs are a family of toxins comprising >20 analogs, which are structurally divided into two groups: CTX3C type and CTX4A type. Compared to previous studies on *G. polynesiensis* strains from French Polynesia or the Cook Islands, the New-Caledonian strain exhibited a low CTX diversity, with no toxins from the CTX3C group (Yon et al., 2021a; Darius et al., 2022; Murray et al., 2024). In the study by Darius et al. (2022) (Darius et al., 2022), the CTX profiles of four *G. polynesiensis* strains from different archipelagos in French Polynesia was determined by LC-MS/MS. Similarly, Murray et al. (2024) (Murray et al., 2024) investigated two *G. polynesiensis* strains isolated from the Cook Islands. None of the strains from these studies showed a CTX profile similar to that the New-Caledonian strain, which contained only CTX4A and CTX4B as the major CTXs. In fact, the main CTXs in Polynesian strains belong to the CTX3C type, with only trace amount of CTX4A type.

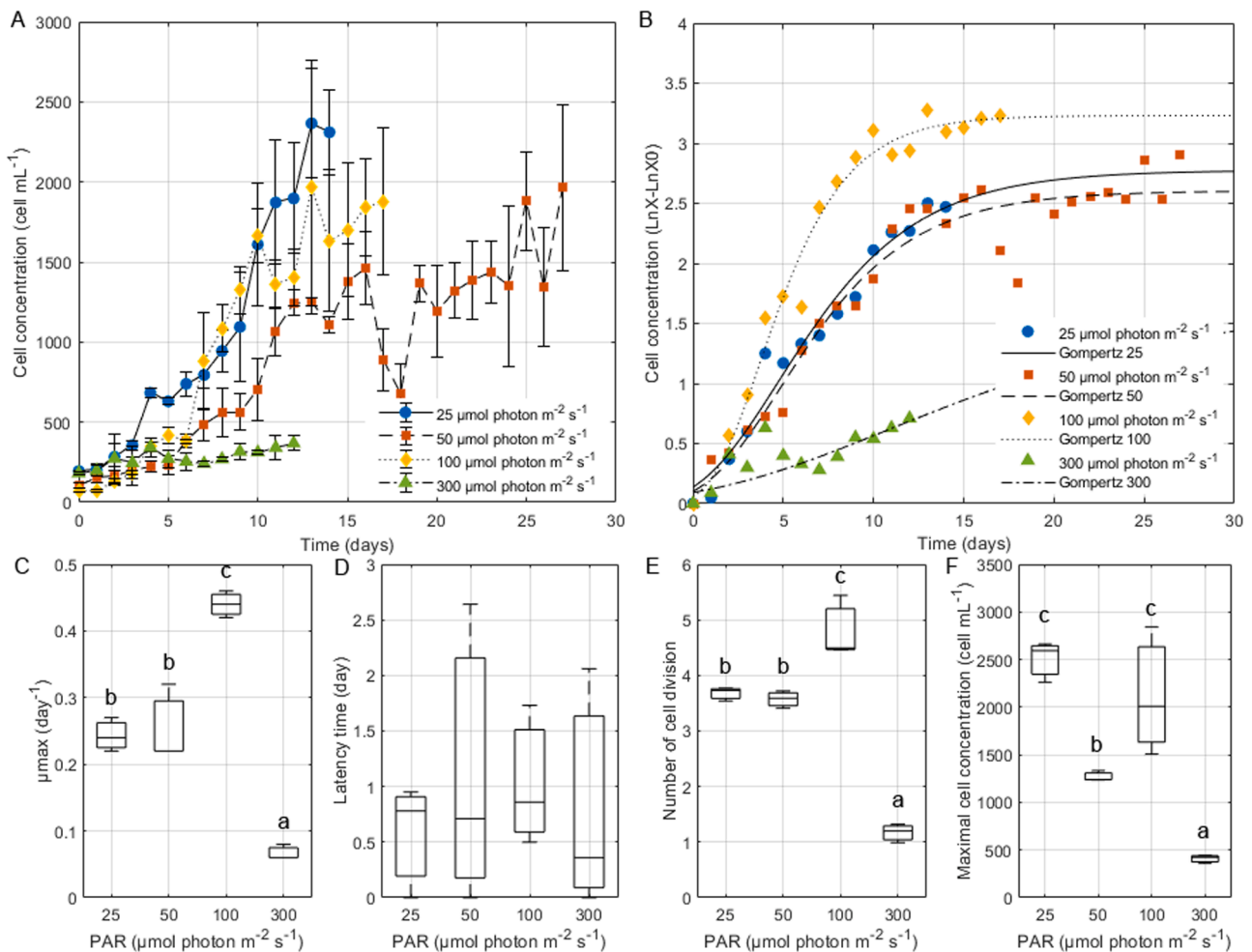


Fig. 7. General growth characteristics: A. Growth curves as a function of time for *Gambierdiscus polyneisensis* at different photosynthetic active radiation (mean ± SD, n = 3). B. Gompertz model fitted to cell concentration as a function of time for the different conditions. C. box plot of the maximum growth rate (μ_{max}) in day⁻¹. D. box plot of the latency time (λ , day). E. box plot of the total number of cell divisions during the experiment; F. box plot of the maximal cell concentration (cell mL⁻¹) obtained in each condition.

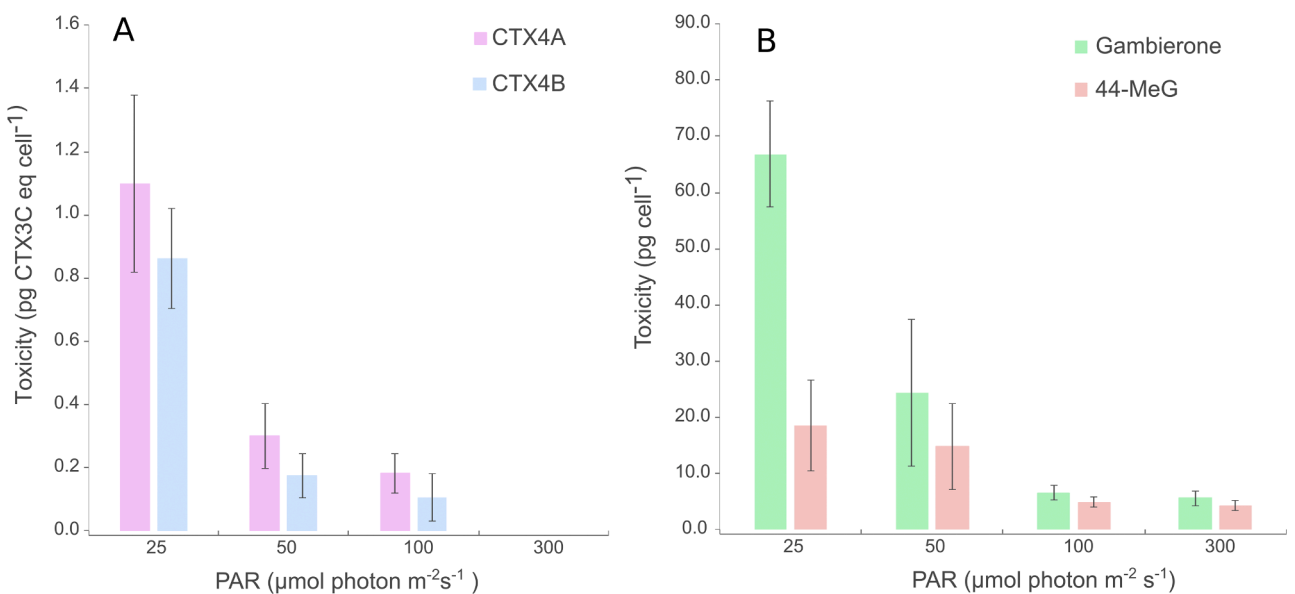


Fig. 8. Toxin concentrations of *Gambierdiscus polyneisensis* at different photosynthetic active radiation (PAR). Average concentrations of CTX4A, CTX4B (A), gambierone and 44-Me-gambierone (B) detected by LC-MS/MS (mean ± SD, n = 3).

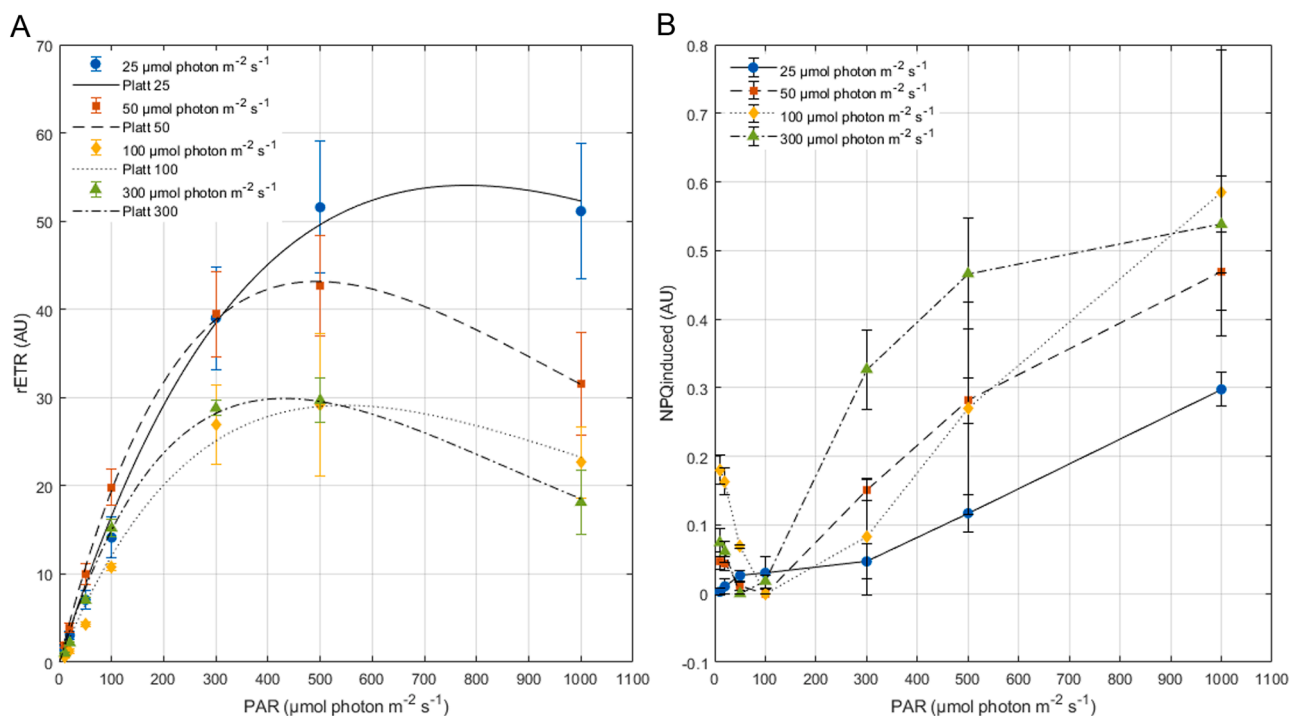


Fig. 9. A. Rapid light curves (RLC, $n = 3$) expressed as the relative electron transport rate (rETR) as a function of the photosynthetic active radiation (PAR in $\mu\text{mol photons m}^{-2} \text{s}^{-1}$) of *Gambierdiscus polynesiensis* exposed to the different irradiance. B. Non photochemical quenching induced (NPQinduced) by the RLCs.

Noticeable amounts of gambierone and 44-MeG were also observed in the strain 19PV93, which is consistent with previous studies (Longo et al., 2019; Rhodes et al., 2023; Murray et al., 2024). Indeed, these toxins have already been reported in *G. polynesiensis*, in four strains from French Polynesia (Longo et al., 2019), two strains from the Cook Islands (Murray et al., 2024), and two additional strains from the Kermadec Islands (Rhodes et al., 2023). Although concentrations were strain-dependent, gambierone was consistently detected in higher amounts than 44-MeG in *G. polynesiensis*. Initially, 44-MeG was characterized in *G. belizeanus* (Boente-Juncal et al., 2019), but since then, it has been detected in 13 *Gambierdiscus* species out of the 19 described (Murray et al., 2024), as well as in two *Fukuyoa* and two *Coolia* (Murray et al., 2020; Tibirica et al., 2020). Similarly, no MTXs were detected (Longo et al., 2019; Yon et al., 2021a).

These results confirm the intraspecific variations in toxin profiles between strains from distinct geographic origins and highlight the need to carefully characterize both toxin profiles and species from CP regions.

4.2. Response to light intensity

Factors governing toxin content in the genera *Gambierdiscus* and *Fukuyoa* still need clarification, especially regarding the role played by environmental and/or physiological drivers and, genetic characteristics. Early laboratory studies have primarily investigated *Gambierdiscus* sp. optima and limits for temperature, salinity and light factors (Kibler et al., 2012; Chinain et al., 2020). Globally, *Gambierdiscus* spp. are able to grow in shaded as well as water habitats exhibiting high light levels (Tester et al., 2013).

In shallow tropical habitats, *Gambierdiscus* spp. are often found attached to benthic macrophytes or coral rubbles where irradiances can sometimes exceed $2000 \mu\text{mol photons m}^{-2} \text{s}^{-1}$ (Villareal and Morton, 2002). Ecophysiological studies, however, highlight that *Gambierdiscus* seem to be best adapted to relatively LL ($50\text{--}230 \mu\text{mol photons m}^{-2} \text{s}^{-1}$) and can even sustain growth at irradiances as low as $10 \mu\text{mol photons m}^{-2} \text{s}^{-1}$, which would allow cells to survive at depths below 80 m in tropical environments (Kibler et al., 2012; Yoshimatsu et al., 2016;

Leynse et al., 2017). The present study confirms these findings and demonstrates that for *G. polynesiensis*, strain 19PV93, typical growth curves can be observed, in batch-culture conditions, at the different conditions of irradiance tested, with the exception of $300 \mu\text{mol photons m}^{-2} \text{s}^{-1}$ where no growth was observed even if the algal cells were still alive. However, growth parameters, such as μ_{max} , showed that an optimum for growth was observed at a medium light intensity ($100 \mu\text{mol photons m}^{-2} \text{s}^{-1}$); whereas, lower growth rate were found at lowest light intensities (25 and $50 \mu\text{mol photons m}^{-2} \text{s}^{-1}$). It is thus similar than for most *Gambierdiscus* species experimentally studied, as optimal species-specific growth rates typically occurred between $\sim 25\text{--}150 \mu\text{mol photons m}^{-2} \text{s}^{-1}$ (Kibler et al., 2012; Xu et al., 2016; Yoshimatsu et al., 2016; Leynse et al., 2017).

In addition to the growth response to light intensity, this study also assesses the response on toxin content and profiles. Interestingly, the response was different than for growth, the impact of light on CTX and gambierone concentrations was found to be inversely correlated to light intensity, as at LL higher CTXs and gambierone concentrations were found compared to HL. Similar observations were made with *G. carpenteri*, where the highest toxin content was observed between 40 and $70 \mu\text{mol photons m}^{-2} \text{s}^{-1}$ (Vacarizas et al., 2018). In addition, of the atypical cell profile of this new strain, which consisted solely of CTX4A and CTX4B, the concentration was found to range from $0.29 \pm 0.13 \text{ pg CTX3C eq cell}^{-1}$ at ML to $1.96 \pm 0.44 \text{ pg CTX3C eq cell}^{-1}$ which places this strain in the low to medium toxicity range (Darius et al., 2022). Toxin concentrations per cell in the light response experiment are significantly higher than those observed in the initial analyses of the *G. polynesiensis* culture (cf 3.2). Indeed, they are 10 to 70 times more toxic than during the early stages of culture following its isolation. In addition, of the impact of the light intensity, that clearly has a significant impact on the toxin content (present study and (Vacarizas et al., 2018). This outcome is not entirely surprising as previous studies have reported that *Gambierdiscus* cultures require extended acclimation period. Indeed, (Bomber et al., 1989a) emphasized the importance of allowing isolates sufficient time to adapt to ambient conditions before achieving maximal toxin production in culture. Similarly, it was claimed that acclimation

periods ranging from 16 weeks to 1 year are typically required for *Gambierdiscus* isolates to fully adapt (Bomber et al., 1989b). In the present case, the strain was isolated in September 2019, and the experiments were conducted in autumn 2022, three years later. Therefore, it is highly unlikely that the differences in toxin content were influenced by the age of the isolates in culture.

Based on previous studies, the total amount of P-CTXs quantified by LC-MS/MS in strains of *G. polynesiensis* ranges from 0 to 11 pg cell⁻¹ (Chinain et al., 2010a; Rhodes et al., 2016; Longo et al., 2019; Rhodes et al., 2023; Murray et al., 2024). The strain 19PV93 from NC is placed in the low to medium toxicity range depending on the light conditions, underlining the need to further investigate the factors influencing *Gambierdiscus* growth and toxin production. Although the total CTX concentrations of this strain are within the range (0 to 11 pg cell⁻¹), its toxin profile shows higher concentration in CTX4A and CTX4B compared to other *G. polynesiensis* strains (Longo et al., 2019; Darius et al., 2022; Murray et al., 2024). This raises concerns regarding public health risks, as these toxins can quickly oxidize into the highly potent CTX1B when assimilated by predators such as carnivorous fish (Yasumoto and Satake, 1996; Yogi et al., 2011). New Caledonia is recognized as a ciguatera-prone region, with a significant prevalence of poisoning cases. A 2005 study indicated that 37.8 % of the adult population in Nouméa had experienced ciguatera poisoning at least once in their lifetime (Baumann et al., 2010). Several hotspots have been identified, including Lifou Island, Isle of Pines, Thio, and Poya on Grande Terre. Additionally, >45 commonly consumed fish species have been reported as carriers of ciguatera (Baumann et al., 2010; DASS, 2017).

Similarly to previous results (Chinain et al., 2010a), our study observed that under slow-growing conditions, *G. polynesiensis* exhibited the highest levels of toxicity, supporting the hypothesis that slower growth rates may induce higher toxin content, as it has been observed in other dinoflagellate species (Jaufrais et al., 2013).

To evaluate the photo-physiological fitness of *G. polynesiensis* under varying light intensities, photosynthetic efficiency was assessed using chlorophyll a fluorescence measurements through PAM fluorometry, combining two methods: RLCs (Ralph and Gademann, 2005; Perkins et al., 2006) and the OJIP tests (Strasser and Strasser, 1995; Strasser et al., 2000). While RLCs serve as a reliable indicator of photosynthetic efficiency at increasing light intensity (Ralph and Gademann, 2005; Perkins et al., 2006); rapid fluorescence induction provides insight into the redox state of the PSII reaction center (RCII) during a short saturating flash, reflecting the primary processes of photosynthesis by monitoring the electron transfer (Strasser and Strasser, 1995).

The maximum quantum efficiency of PSII (Fv/Fm), a key indicator of photosynthetic efficiency, peaked at 50 μmol photons m⁻² s⁻¹ (Fv/Fm = 0.63 ± 0.02) but decreased under both lower (0.45 ± 0.03) and higher light conditions (0.30 ± 0.02 and 0.16 ± 0.03 at HL, Table 2). *Gambierdiscus* species are known for their highly variable Fv/Fm values, which are sensitive to light acclimation (Villareal and Morton, 2002; Leynse et al., 2017).

To gain further insights, RLCs were used to assess the ability of *G. polynesiensis* to utilize light intensities ranging from 0 to 1000 μmol photons m⁻² s⁻¹ under the different culture conditions. Under all tested conditions, RLCs exhibited three distinct phases: an initial increase in the light-limiting linear region, followed by a light-saturating plateau, and then photoinhibition (Ralph and Gademann, 2005). This suggests that *G. polynesiensis* is highly sensitive to light intensity, as indicated by the presence of photo-inhibition and the activation of photoprotective processes. NPQ, a photoprotective mechanism that dissipates excess light as heat (Lacour et al., 2020), was clearly observed and correlated with high light intensity as indicated by the NPQ-induced during the RLCs, but also particularly as a response to the different light conditions (NPQremaining). This highlights that *Gambierdiscus* utilizes NPQ as a photoprotective strategy to efficiently protect PSII from excessive light in the present case during both short and long-term exposure to HL. For

Gambierdiscus, NPQ might help to prevent or minimize photo-inhibition in response to short but also long-term fluctuations in irradiance, maximizing photosynthesis and productivity in the high irradiance of shallow coral reef habitats. However, NPQ alone appears insufficient, as photoinhibition was consistently observed and rETR rapidly declined with increasing light intensity, which highlight potential damages on the photosynthetic chain that mainly result from the ROS-generated oxidative stress that target the PsbA (D1) protein of PSII (Goss and Lepetit, 2015). It also highlights the need for *Gambierdiscus* cells to implement behavioural strategies to cope with light, as previously mentioned in the literature (Bomber et al., 1988; Morton et al., 1992; Villareal and Morton, 2002; Kibler et al., 2012; Yoshimatsu et al., 2016).

Light acclimation was also evident, as *G. polynesiensis* increased its light-harvesting capacity (indicated by high rETRmax) under LL conditions, while reducing its rETRmax under HL conditions (Fig. 9 and Table 2). Excessive light can also overwhelm NPQ, leading to damage of the D1 protein, a decline in photosynthetic efficiency, chronic photoinhibition, and the production of reactive oxygen species (ROS) (Franklin and Forster, 1997). The observed decline in rETRmax at HL intensity in this study is likely due to the exhaustion/saturation of photoregulation mechanisms (e.g., NPQ), leading to long-term photoinhibition and reduced growth.

This is further confirmed by OJIP tests, where low absorption values by RC (M0) and minimal energy dissipation as heat (DIO/RC) were observed under the LL conditions (25 and 50 μmol photons m⁻² s⁻¹), correlating with high maximum quantum efficiencies of primary photochemistry (φP0 and Fv/Fm). Additionally, in this study, the rate of electron transfer from QA- to PQ per active PSII (ET0/RC) did not seem to be impacted by light intensity, but flux or yield (Ψ0 and φE0) in the electron transport chain were clearly reduced at higher light intensities resulting in a reduced performance index (Pi-abs) at HL intensities.

All these parameters indicate an optimal light intensity for this strain of *Gambierdiscus* situated around 50 μmol photons m⁻² s⁻¹, as illustrated by the high Pi-abs. Above this intensity, photoprotective mechanisms are implemented and become insufficient at light intensities above 100 μmol photons m⁻² s⁻¹, compromising growth and toxin content.

5. Conclusion

This study describes a new strain of *Gambierdiscus polynesiensis* (19PV93) isolated from the west coast of New Caledonia. It exhibited the presence of gambierone, 44-MeG, and an atypical CTX profile (CTX4A and CTX4B), highlighting intraspecific toxin variations across different regions. In culture, *G. polynesiensis* preferred lower light intensities (50–100 μmol photons m⁻² s⁻¹) and showed higher CTX and gambierone content at low levels (25 μmol photons m⁻² s⁻¹). The species efficiently employs non-photochemical quenching (NPQ) to protect PSII from excess light, but this mechanism alone proved to be insufficient as photoinhibition and reduced electron transfer were rapidly observed at higher light intensities.

CRedit authorship contribution statement

Manoëlla Sibat: Writing – review & editing, Writing – original draft, Methodology, Investigation, Funding acquisition, Formal analysis, Data curation, Conceptualization. **Tepoerau Mai:** Writing – review & editing, Formal analysis. **Nicolas Chomérat:** Writing – review & editing, Methodology, Investigation, Funding acquisition, Data curation, Conceptualization. **Gwenael Bilien:** Writing – review & editing, Formal analysis, Data curation. **Korian Lhaute:** Writing – review & editing, Methodology, Formal analysis. **Philipp Hess:** Writing – review & editing. **Véronique Séchet:** Writing – review & editing, Methodology. **Thierry Jauffrais:** Writing – review & editing, Writing – original draft, Methodology, Investigation, Funding acquisition, Data curation, Conceptualization.

Declaration of competing interest

The authors declare that they have no known competing financial interests or personal relationships that could have appeared to influence the work reported in this paper.

Acknowledgements

The authors acknowledge Ifremer for supporting the Maorix and Coconut project (Ifremer core funding), the French National Research Agency (France 2030, ANR-23-POCE-0001, project MaHeWa), the South Province of New Caledonia who delivered the sampling authorizations (20274–2019/2-ISP/DENV) and the Sue Tai Ocean Fellowship for TM postdoctoral fellowship.

For the SEM images, this work has benefited from the facilities of P2M with the technical assistance of Aurélie Monnin and Olivia Barthelemy, Université de la Nouvelle Calédonie.

Supplementary materials

Supplementary material associated with this article can be found, in the online version, at [doi:10.1016/j.hal.2025.102859](https://doi.org/10.1016/j.hal.2025.102859).

Data availability

Data will be made available on request.

References

- Adachi, R., Fukuyo, Y., 1979. The thecal structure of a toxic marine dinoflagellate *Gambierdiscus toxicus* gen. Et spec. nov. Collected in a ciguatera-endemic area. Bull. Jpn. Soc. Sci. Fish. 45, 67–71.
- Andrefouet, S., Cabioch, G., Flamand, B., Pelletier, B., 2009. A reappraisal of the diversity of geomorphological and genetic processes of New Caledonian coral reefs: a synthesis from optical remote sensing, coring and acoustic multibeam observations. Coral Reefs. 28, 691–707.
- Bagnis, R., Chanteau, S., Chungue, E., Hurtel, J.M., Yasumoto, T., Inoue, A., 1980. Origins of ciguatera fish poisoning - a new dinoflagellate, *Gambierdiscus toxicus* adachi and *Fukuyo*, definitively involved as a causal agent. Toxicol. 18 (2), 199–208.
- Baumann, F., Bourrat, M.-B., Pauillac, S., 2010. Prevalence, symptoms and chronicity of ciguatera in New Caledonia: results from an adult population survey conducted in Noumea during 2005. Toxicol. 56, 662–667.
- Boente-Juncal, A., Alvarez, M., Antelo, A., Rodriguez, I., Calabro, K., Vale, C., Thomas, O. P., Botana, L.M., 2019. Structure elucidation and biological evaluation of maitotoxin-3, a homologue of Gambierone, from *Gambierdiscus belizeanus*. Toxins. (Basel) 11 (2).
- Boisnoir, A., Pascal, P.Y., Cordonnier, S., Leme, R., 2018. Depth distribution of benthic dinoflagellates in the Caribbean Sea. J. Sea. Res. 135, 74–83.
- Bomber, J.W., Guillard, R.R.L., Nelson, W.G., 1988. Roles of temperature, salinity, and light in seasonality, growth, and toxicity of ciguatera-causing *Gambierdiscus toxicus* adachi et *Fukuyo* (dinophyceae). J. Exp. Mar. Biol. Ecol. 115 (1), 53–65.
- Bomber, J.W., Tindall, D.R., Miller, D.M., 1989a. Genetic variability in toxin potencies among seventeen clones of *Gambierdiscus toxicus* (Dinophyceae). J. Phycol. 25 (4), 617–625.
- Bomber, J.W., Tindall, D.R., Venable, C.W., Miller, D.M., 1989b. Pigment Composition and Low-Light Response of 14 Clones of *Gambierdiscus toxicus* 4th International Conf On Toxic Marine Phytoplankton. Elsevier, Univ Lund, Dept Marine Ecol, Lund, Sweden, pp. 263–268.
- Château-Degat, M.L., Beuter, A., Vauterin, G., Nguyen, N.L., Chinain, M., Darius, T., Legrand, A.M., Chansin, R., Dewailly, E., 2007. Neurologic signs of ciguatera disease: evidence of their persistence. Am. J. Trop. Med. Hyg. 77 (6), 1170–1175.
- Chinain, M., Darius, H.T., Ung, A., Cruchet, P., Wang, Z.H., Ponton, D., Laurent, D., Pauillac, S., 2010a. Growth and toxin production in the ciguatera-causing dinoflagellate *Gambierdiscus polynesiensis* (Dinophyceae) in culture. Toxicol. 56 (5), 739–750.
- Chinain, M., Darius, H.T., Ung, A., Fouc, M.T., Revel, T., Cruchet, P., Pauillac, S., Laurent, D., 2010b. Ciguatera risk management in French Polynesia: the case study of Raivavae Island (Australes Archipelago). Toxicol. 56 (5), 674–690.
- Chinain, M., Faust, M.A., Pauillac, S., 1999a. Morphology and molecular analyses of three toxic species of *Gambierdiscus* (Dinophyceae): *G-pacifcus*, sp nov., *G-australes*, sp nov., and *G-polynesiensis*, sp nov. J. Phycol. 35 (6), 1282–1296.
- Chinain, M., Gatti, C., Roue, M., Darius, H.T., 2020. Ciguatera-causing dinoflagellates in the genera *Gambierdiscus* and *Fukuyo*: distribution, ecophysiology and toxicology. In: Subba Rao, D.V. (Ed.), *Dinoflagellates: Classification, Evolution, Physiology and Ecological Significance*. <https://novapublishers.com/wp-content/uploads/2020/09/978-1-53617-888-3.pdf>.
- Chinain, M., Gatti, C.M.I., Darius, H.T., Quod, J.P., Tester, P.A., 2021. Ciguatera poisonings: a global review of occurrences and trends. Harmful. Algae. 102, 101873.
- Chinain, M., Germain, M., Deparis, X., Pauillac, S., Legrand, A.M., 1999b. Seasonal abundance and toxicity of the dinoflagellate *Gambierdiscus* spp (Dinophyceae), the causative agent of ciguatera in Tahiti, French Polynesia. Mar. Biol. 135 (2), 259–267.
- Clua, E., Brena, P.F., Lecasble, C., Ghnassia, R., Chauvet, C., 2011. Prevalence and proposal for cost-effective management of the ciguatera risk in the Noumea fish market, New Caledonia (South Pacific). Toxicol. 58 (6–7), 591–601.
- Conan, P., Joux, F., Torretton, J.P., Pujo-Pay, M., Douki, T., Rochelle-Newall, E., Mari, X., 2008. Effect of solar ultraviolet radiation on bacterio- and phytoplankton activity in a large coral reef lagoon (Southwest New Caledonia). Aquat. Microb. Ecol. 52, 83–98.
- Coulombier, N., Blanchier, P., Le Dean, L., Barthelemy, V., Lebouvier, N., Jauffrais, T., 2021. The effects of CO₂-induced acidification on *Tetraselmis* biomass production, photophysiology and antioxidant activity: a comparison using batch and continuous culture. J. Biotech. 325, 312–324.
- Courtial, L., Roberty, S., Shick, J.M., Houllbrèque, F., Ferrier-Pagès, C., 2017. Interactive effects of ultraviolet radiation and thermal stress on two reef-building corals. Limnol. Ocean. 62, 1000–1013.
- Cuyper, E., Abdel-Mottaleb, Y., Kopljar, I., Rainier, J.D., Raes, A.L., Snyders, D.J., Tytgat, J., 2008. Gambierol, a toxin produced by the dinoflagellate *Gambierdiscus toxicus*, is a potent blocker of voltage-gated potassium channels. Toxicol. 51 (6), 974–983.
- Darius, H.T., Revel, T., Cruchet, P., Viallon, J., Gatti, C.M.I., Sibat, M., Hess, P., Chinain, M., 2021. Deep-water fish are potential vectors of ciguatera poisoning in the Gambier Islands, French Polynesia. Mar. Drugs. 19 (11).
- Darius, H.T., Revel, T., Viallon, J., Sibat, M., Cruchet, P., Longo, S., Hardison, D.R., Holland, W.C., Tester, P.A., Litaker, R.W., McCall, J.R., Hess, P., Chinain, M., 2022. Comparative study on the performance of three detection methods for the quantification of pacific ciguatoxins in French polynesian strains of *Gambierdiscus polynesiensis*. Mar. Drugs.
- Darius, H.T., Roué, M., Sibat, M., Viallon, J., Gatti, C.M.I., Vandersea, M.W., Tester, P., Litaker, R.W., Amzil, Z., Hess, P., Chinain, M., 2018. Toxicological investigations on the sea urchin *Triploneustes gratilla* (Toxopneustidae, Echinoid) from Anaho Bay (Nuku Hiva, French Polynesia): evidence for the presence of Pacific ciguatoxins. Mar. Drugs.
- Darius, H.T., Roué, M., Sibat, M., Viallon, J., Gatti, C.M.I., Vandersea, M.W., Tester, P.A., Litaker, R.W., Amzil, Z., Hess, P., Chinain, M., 2017. Tectus niloticus (Tegulidae, Gastropod) as a novel vector of ciguatera poisoning: detection of pacific ciguatoxins in toxic samples from Nuku Hiva Island (French Polynesia). Toxins. (Basel) 10 (1).
- Diogene, J., Reverte, L., Rambla-Alegre, M., Del Rio, V., de la Iglesia, P., Campas, M., Palacios, O., Flores, C., Caixach, J., Ralijaona, C., Razaanajato, I., Pirog, A., Magalon, H., Arnich, N., Turquet, J., 2017. Identification of ciguatoxins in a shark involved in a fatal food poisoning in the Indian Ocean. Sci. Rep. 7 (1), 8240.
- Estevez, P., Castro, D., Leao-Martins, J.M., Sibat, M., Tudo, A., Dickey, R., Diogene, J., Hess, P., Gago-Martinez, A., 2021. Toxicity screening of a *Gambierdiscus* australes strain from the Western Mediterranean Sea and identification of a novel maitotoxin analogue. Mar. Drugs. 19 (8).
- Estevez, P., Sibat, M., Leao-Martins, J.M., Tudo, A., Rambla-Alegre, M., Aligizaki, K., Diogene, J., Gago-Martinez, A., Hess, P., 2020. Use of mass spectrometry to determine the diversity of toxins produced by *Gambierdiscus* and *Fukuyo* species from Balearic Islands and Crete (Mediterranean Sea) and the Canary Islands (Northeast Atlantic). Toxins. (Basel) 12 (5).
- Franklin, L.A., Forster, R.M., 1997. The changing irradiance environment: consequences for marine macrophyte physiology, productivity and ecology. Eur. J. Phycol. 32 (3), 207–232.
- Friedman, M.A., Fernandez, M., Backer, L.C., Dickey, R.W., Bernstein, J., Schrank, K., Kibler, S., Stephan, W., Gribble, M.O., Bienfang, P., Bowen, R.E., Degrasse, S., Quintana, H.A.F., Loeffler, C.R., Weisman, R., Blythe, D., Berdalet, E., Ayyar, R., Clarkston-Townsend, D., Swajian, K., Benner, R., Brewer, T., Fleming, L.E., 2017. An updated review of ciguatera fish poisoning: clinical, epidemiological, environmental, and public health management. Mar. Drugs. 15 (3).
- Fukuyo, A., 1981. Taxonomical study on benthic dinoflagellates collected in coral reefs. Bull. Jpn. Soc. Sci. Fish. 47 (8), 967–978.
- Funaki, H., Nishimura, T., Yoshioka, T., Ataka, T., Tani, Y., Hashimoto, K., Yamaguchi, H., Adachi, M., 2022. Toxicity and growth characteristics of epiphytic dinoflagellate *Gambierdiscus silvae* in Japan. Harmful. Algae. 115, 102230.
- Gomez, F., Qiu, D.J., Lopes, R.M., Lin, S.J., 2015. *Fukuyo paulensis* gen. Et sp nov., a new genus for the globular species of the dinoflagellate *Gambierdiscus* (Dinophyceae). PLoS. One. 10 (4).
- Goss, R., Lepetit, B., 2015. Biodiversity of NPQ. J. Plant. Physiol. 172, 13–32.
- Guindon, S., Dufayard, J.F., Lefort, V., Anisimova, M., Hordijk, W., Gascuel, O., 2010. New algorithms and methods to estimate maximum-likelihood phylogenies: assessing the performance of PhyML 3.0. Syst. Biol. 59 (3), 307–321.
- Hamilton, B., Hurbungs, M., Jones, A., Lewis, R.J., 2002. Multiple ciguatoxins present in Indian Ocean reef fish. Toxicol. 40 (9), 1347–1353.
- Holmes, M.J., 1998. *Gambierdiscus yasumotoi* sp. nov. (Dinophyceae), a toxic benthic dinoflagellate from Southeastern Asia. J. Phycol. 34 (4), 661–668.
- Holmes, M.J., Lewis, R.J., Gillespie, N.C., 1990. Toxicity of Australian and French Polynesian strains of *Gambierdiscus Toxicus* (Dinophyceae) grown in culture: characterization of a new type of maitotoxin. Toxicol. 28 (10), 1159–1172.
- Holmes, M.J., Lewis, R.J., Poli, M.A., Gillespie, N.C., 1991. Strain dependent production of ciguatoxin precursors (*Gambierdiscus toxicus*) by *Gambierdiscus toxicus* (Dinophyceae) in culture. Toxicol. 29, 761–775.
- Direction des Affaires Sanitaires et Sociales, DASS, 2017. Situation sanitaire en Nouvelle-Calédonie.

- Hoppenrath, M., Murray, S., Chomérat, N., Horiguchi, T., 2014. Marine benthic dinoflagellates - unveiling their worldwide biodiversity.
- Hossen, V., Velge, P., Turquet, J., Chinain, M., Laurent, D., Krys, S., 2013. La ciguatera: un état des lieux en France et dans l'Union européenne. *Bull. Épidémiol. Santé Anim. Aliment.* 56, 3–9.
- Jauffrais, T., Agogue, H., Gemin, M.-P., Beaugeard, L., Martin-Jézéquel, V., 2017. Effect of bacteria on growth and biochemical composition of two benthic diatoms *Halamphora coffeaeformis* and *Entomoneis paludosa*. *J. Exp. Mar. Biol. Ecol.* 495, 65–74.
- Jauffrais, T., Brisset, M., Lagourgue, L., Payri, C.E., Gobin, S., Le Gendre, R., Van Wynsberge, S., 2022. Seasonal changes in the photophysiology of *Ulva batuffolosa* in a coastal barrier reef. *Aquat. Bot.*, 103515.
- Jauffrais, T., Séchet, V., Herrenknecht, C., Truquet, P., Savar, V., Tillmann, U., Hess, P., 2013. Effect of environmental and nutritional factors on growth and azaspiracid production of the dinoflagellate *Azadinium spinosum*. *Harmful. Algae.* 27, 138–148.
- Katoh, K., Standley, D.M., 2013. MAFFT multiple sequence alignment software version 7: improvements in performance and usability. *Mol. Biol. Evol.* 30 (4), 772–780.
- Kibler, S.R., Litaker, R.W., Holland, W.C., Vandersea, M.W., Tester, P.A., 2012. Growth of eight *Gambierdiscus* (Dinophyceae) species: effects of temperature, salinity and irradiance. *Harmful. Algae.* 19, 1–14.
- Kirk, J.T.O., 1994. *Light and Photosynthesis in Aquatic Ecosystems*, 2 ed. Cambridge University Press, Cambridge.
- Kryuchkov, F., Robertson, A., Miles, C.O., Mudge, E.M., Uhlig, S., 2020. LC-HRMS and Chemical derivatization strategies for the structure elucidation of caribbean ciguatoxins: identification of C-CTX-3 and -4. *Mar. Drugs.* 18 (4).
- Lacour, T., Babin, M., Lavaud, J., 2020. Diversity in xanthophyll cycle pigments content and related nonphotochemical quenching (NPQ) among microalgae: implications for growth strategy and ecology. *J. Phycol.* 56 (2), 245–263.
- Lewis, R.J., Holmes, M.J., 1993. Origin and transfer of toxins involved in ciguatera. *Comp. Biochem. Physiol. C. Comp. Pharmacol. Toxicol.* 106 (3), 615–628.
- Leynse, A.K., Parsons, M.L., Thomas, S.E., 2017. Differences in the photoacclimation and photoprotection exhibited by two species of the ciguatera causing dinoflagellate genus, *Gambierdiscus*. *Harmful. Algae.* 70, 90–97.
- Litaker, R.W., Vandersea, M.W., Faust, M.A., Kibler, S.R., Chinain, M., Holmes, M.J., Holland, W.C., Tester, P.A., 2009. Taxonomy of *Gambierdiscus* including four new species, *Gambierdiscus caribaeus*, *Gambierdiscus carolinianus*, *Gambierdiscus carpenteri* and *Gambierdiscus ruetzleri* (Gonyaulacales, Dinophyceae). *Phycologia.* 48 (5), 344–390.
- Litaker, R.W., Vandersea, M.W., Faust, M.A., Kibler, S.R., Nau, A.W., Holland, W.C., Chinain, M., Holmes, M.J., Tester, P.A., 2010. Global distribution of ciguatera causing dinoflagellates in the genus *Gambierdiscus*. *Toxicon.* 56 (5), 711–730.
- Longo, S., Sibat, M., Viallon, J., Darius, H.T., Hess, P., Chinain, M., 2019. Intraspecific variability in the toxin production and toxin profiles of *In vitro* cultures of *Gambierdiscus polynesiensis* (Dinophyceae) from French Polynesia. *Toxins.* (Basel) 11 (12).
- Meriot, V., Rousset, A., Brunet, N., Chomerat, N., Bilien, G., Le Dean, L., Berteaux-Lecellier, V., Coulombier, N., Lebouvier, N., Jauffrais, T., 2024. *Heterocapsa cf. bohaisensis* (dinoflagellate): identification and response to nickel and iron stress revealed through chlorophyll *a* fluorescence. *Photosynthetica*.
- Morton, S.L., Norris, D.R., Bomber, J.W., 1992. Effect of temperature, salinity and light-intensity on the growth and seasonality of toxic dinoflagellates associated with ciguatera. *J. Exp. Mar. Biol. Ecol.* 157 (1), 79–90.
- Mudge, E.M., Miles, C.O., Ivanova, L., Uhlig, S., James, K.S., Erdner, D.L., Fæste, C.K., McCarron, P., Robertson, A., 2023. Algal ciguatoxin identified as source of ciguatera poisoning in the Caribbean. *Chemosphere.* 330, 138659.
- Murata, M., Yasumoto, T., 1995. Structure of Maitotoxin, the most toxic and largest natural non-biopolymer. *J. Synth. Org. Chem. Jpn.* 53 (3), 207–217.
- Murray, J.S., Finch, S.C., Harwood, D.T., Mudge, E.M., Wilkins, A.L., Puddick, J., Rhodes, L.L., Ginkel, R.V., Rise, F., Prinsep, M.R., 2022. Structural characterization of maitotoxins produced by toxic gambierdiscus species. *Mar. Drugs.* 20 (453), 1–31.
- Murray, J.S., Nishimura, T., Finch, S.C., Rhodes, L.L., Puddick, J., Harwood, D.T., Larsson, M.E., Doblin, M.A., Leung, P., Yan, M., Rise, F., Wilkins, A.L., Prinsep, M.R., 2020. The role of 44-methylgambierone in ciguatera fish poisoning: acute toxicity, production by marine microalgae and its potential as a biomarker for *Gambierdiscus* spp. *Harmful. Algae.* 97, 101853.
- Murray, J.S., Passfield, E.M.F., Rhodes, L.L., Puddick, J., Finch, S.C., Smith, K.F., van Ginkel, R., Mudge, E.M., Nishimura, T., Funaki, H., Adachi, M., Prinsep, M.R., Harwood, D.T., 2024. Targeted metabolite fingerprints of thirteen gambierdiscus, five *Coolia* and two *Fukuyoa* species. *Mar. Drugs.* 22 (3), 119.
- Murray, J.S., Selwood, A.I., Harwood, D.T., van Ginkel, R., Puddick, J., Rhodes, L.L., Rise, F., Wilkins, A.L., 2019. 44-Methylgambierone, a New Gambierone Analogue Isolated from *Gambierdiscus* australis. *Tetrahedron Letters*.
- Nagai, H., Mikami, Y., Yazawa, K., Gono, T., Yasumoto, T., 1993. Biological activities of novel polyether antifungals, gambieric acids A and B from a marine dinoflagellate *gambierdiscus toxicus*. *J. Antibiot. (Tokyo)* 46 (3), 520–522.
- Nguyen-Ngoc, L., Larsen, J., Doan-Nhu, H., Nguyen, X.-V., Chomérat, N., Lundholm, N., Phan-Tan, L., Dao, H.V., Nguyen, N.-L., Nguyen, H.-H., Van Chu, T., 2023. *Gambierdiscus* (Gonyaulacales, Dinophyceae) diversity in Vietnamese waters with description of *G. vietnamensis* sp. nov. *J. Phycol.* 59 (3), 496–517.
- Nunn, G.B., Theisen, B.F., Christensen, B., Arcander, P., 1996. Simplicity-correlated size growth of the nuclear 28S ribosomal RNA D3 expansion segment in the crustacean order Isopoda. *J. Mol. Evol.* 42 (2), 211–223.
- Oshiro, N., Nagasawa, H., Kuniyoshi, K., Kobayashi, N., Sugita-Konishi, Y., Asakura, H., Yasumoto, T., 2021. Characteristic distribution of ciguatoxins in the edible parts of a grouper, *Variola louti*. *Toxins.* (Basel) 13 (3).
- Oshiro, N., Nagasawa, H., Nishimura, M., Kuniyoshi, K., Kobayashi, N., Sugita-Konishi, Y., Ikehara, T., Tachihara, K., Yasumoto, T., 2023. Analytical studies on ciguateric fish in Okinawa, Japan (II): the grouper *Variola albimarginata*. *J. Mar. Sci. Eng.* 11 (2), 1–13.
- Perkins, R.G., Mouget, J.L., Lefebvre, S., Lavaud, J., 2006. Light response curve methodology and possible implications in the application of chlorophyll fluorescence to benthic diatoms. *Mar. Biol.* 149 (4), 703–712.
- Pisapia, F., Sibat, M., Watanabe, R., Roullier, C., Suzuki, T., Hess, P., Herrenknecht, C., 2020. Characterization of maitotoxin-4 (MTX4) using electrospray positive mode ionization high-resolution mass spectrometry and UV spectroscopy. *Rapid. Commun. Mass. Spectrom.* 34 (19).
- Platt, T., Gallegos, C.L., Harrison, W.G., 1980. Photoinhibition of photosynthesis in natural assemblages of marine phytoplankton. *J. Mar. Res.* 38, 687–701.
- Pringault, O., de Wit, R., Camoin, G., 2005. Irradiance regulation of photosynthesis and respiration in modern marine microbialites built by benthic cyanobacteria in a tropical lagoon (New Caledonia). *Microb. Ecol.* 49, 604–616.
- Ralph, P.J., Gademann, R., 2005. Rapid light curves: a powerful tool to assess photosynthetic activity. *Aquat. Bot.* 82 (3), 222–237.
- Rhodes, L.L., Smith, K.F., Murray, J.S., Passfield, E.M.F., D'Archino, R., Nelson, W., Nishimura, T., Thompson, L., Trnski, T., 2023. Sub-tropical benthic/epiphytic dinoflagellates of Aotearoa New Zealand and Rangitāhua Kermadec Islands. *Harmful. Algae.* 128, 102494.
- Rhodes, L.L., Smith, K.F., Verma, A., Murray, S., Harwood, D.T., Trnski, T., 2016. The dinoflagellate genera gambierdiscus and ostreopsis from subtropical Raoul Island and North Meyer Island, Kermadec Islands. *N. Z. J. Mar. Freshw. Res.* 51 (4), 490–504.
- Rodriguez, I., Genta-Jouve, G., Alfonso, C., Calabro, K., Alonso, E., Sanchez, J.A., Alfonso, A., Thomas, O.P., Botana, L.M., 2015. Gambierone, a ladder-shaped polyether from the dinoflagellate *Gambierdiscus belizeanus*. *Org. Lett.* 17 (10), 2392–2395.
- Ronquist, F., Huelsenbeck, J.P., 2003. MrBayes 3: bayesian phylogenetic inference under mixed models. *Bioinform.* 19 (12), 1572–1574.
- Roué, M., Darius, H.T., Picot, S., Ung, A., Viallon, J., Gaertner-Mazouni, N., Sibat, M., Amzil, Z., Chinain, M., 2016. Evidence of the bioaccumulation of ciguatoxins in giant clams (*Tridacna maxima*) exposed to *Gambierdiscus* spp. *Cells. Harmful. Algae.* 57, 78–87.
- Sanagi, M.M., Ling, S.L., Nasir, Z., Ibrahim, W.A.W., Abu, A., 2009. Comparison of signal-to-noise, blank determination, and linear regression methods for the estimation of detection and quantification limits for volatile organic compounds by gas chromatography. *J. AOAC Int.* 92 (6), 1833–1838.
- Schneider, C.A., Rasband, W.S., Eliceiri, K.W., 2012. NIH image to ImageJ: 25 years of image analysis. *Nat. Method.* 9 (7), 671–675.
- Scholín, C.A., Villac, M.C., Buck, K.R., Krupp, J.M., Powers, D.A., Fryxell, G.A., Chavez, F.P., 1994. Ribosomal DNA sequences discriminate among toxic and non-toxic *Pseudonitzschia* species. *Nat. Toxins.* 2, 152–165.
- Serodio, J., Cruz, S., Vieira, S., Brotas, V., 2005. Non-photochemical quenching of chlorophyll fluorescence and operation of the xanthophyll cycle in estuarine microphytobenthos. *J. Exp. Mar. Biol. Ecol.* 326 (2), 157–169.
- Sibat, M., Herrenknecht, C., Darius, H.T., Roué, M., Chinain, M., Hess, P., 2018. Detection of pacific ciguatoxins using liquid chromatography coupled to either low or high resolution mass spectrometry (LC-MS/MS). *J. Chromatogr. A*.
- Strasser, B., Strasser, R., 1995. Measuring fast fluorescence transients to address environmental questions: the JIP-test. In: Mathis, P. (Ed.), *Photosynthesis: From Light to Biosphere*. Kluwer Academic Publishers, Dordrecht, pp. 977–980.
- Strasser, R., Srivastava, A., Tsimilli-Michael, M., 2000. The fluorescence transient as a tool to characterize and screen photosynthetic samples. In: *Probing photosynthesis: Mechanism, regulation and adaptation*.
- Tester, P.A., Vandersea, M.W., Buckel, C.A., Kibler, S.R., Holland, W.C., Davenport, E.D., Clark, R.D., Edwards, K.F., Taylor, J.C., Vander Pluym, J.L., Hickerson, E.L., Litaker, R.W., 2013. *Gambierdiscus* (Dinophyceae) species diversity in the Flower Garden Banks National Marine Sanctuary, Northern Gulf of Mexico, USA. *Harmful. Algae.* 29, 1–9.
- Tibirica, C., Sibat, M., Fernandes, L.F., Bilien, G., Chomerat, N., Hess, P., Mafra Jr., L.L., 2020. Diversity and toxicity of the genus *Coolia* Meunier in Brazil, and detection of 44-methyl Gambierone in *Coolia* tropicalis. *Toxins.* (Basel) 12 (5).
- Torregiani, J.H., Lesser, M.P., 2007. The effects of short-term exposures to ultraviolet radiation in the Hawaiian Coral *Montipora verrucosa*. *J. Exp. Mar. Biol. Ecol.* 340, 194–203.
- Vacarizas, J., Benico, G., Austero, N., Azanza, R., 2018. Taxonomy and toxin production of gambierdiscus carpenteri (Dinophyceae) in a tropical marine ecosystem: the first record from the Philippines. *Mar. Pollut. Bull.* 137, 430–443.
- Vernoux, J.-P., Lewis, R.J., 1997. Isolation and characterisation of Caribbean ciguatoxins from the horse-eye jack (*Caranx latus*). *Toxicon.* 35 (6), 889–900.
- Vial, J., Jardy, A., 1999. Experimental comparison of the different approaches to estimate LOD and LOQ of an HPLC method. *Anal. Chem.* 71 (14), 2672–2677.
- Villareal, T.A., Morton, S.L., 2002. Use of cell-specific PAM-fluorometry to characterize host shading in the epiphytic dinoflagellate *gambierdiscus toxicus*. *Mar. Ecol.-Publ. Stn. Zool. Napoli.* 23 (2), 127–140.
- Watanabe, R., Uchida, H., Suzuki, T., Matsushima, R., Nagae, M., Toyohara, Y., Satake, M., Oshima, Y., Inoue, A., Yasumoto, T., 2013. Gambieroxide, a novel epoxy polyether compound from the dinoflagellate *Gambierdiscus toxicus* GTP2 strain. *Tetrahedron.* 69 (48), 10299–10303.
- Xu, Y.X., Richlen, M.L., Liefer, J.D., Robertson, A., Kulis, D., Smith, T.B., Parsons, M.L., Anderson, D.M., 2016. Influence of environmental variables on Gambierdiscus spp. (Dinophyceae) Growth and distribution. *PLoS. One.* 11 (4).

- Yasumoto, T., 2001. The chemistry and biological function of natural marine toxins. *Chem. Rec.* 1, 228–242.
- Yasumoto, T., Satake, M., 1996. Chemistry, etiology and determination methods of ciguatera toxins. *J. Toxicol.-Toxin Rev.* 15 (2), 91–107.
- Yogi, K., Oshiro, N., Inafuku, Y., Hiram, M., Yasumoto, T., 2011. Detailed LC-MS/MS analysis of ciguatoxins revealing distinct regional and species characteristics in fish and causative alga from the Pacific. *Anal. Chem.* 83 (23), 8886–8891.
- Yogi, K., Oshiro, N., Matsuda, S., Sakugawa, S., Matsuo, T., Yasumoto, T., 2013. Toxin profiles in fish implicated in ciguatera fish poisoning in Amami and Kakeroma Islands, Kagoshima Prefecture, Japan. *Food Hyg. Saf. Sci.* 54 (6), 385–391.
- Yon, T., Sibat, M., Reveillon, D., Bertrand, S., Chinain, M., Hess, P., 2021a. Deeper insight into *Gambierdiscus polynesiensis* toxin production relies on specific optimization of high-performance liquid chromatography-high resolution mass spectrometry. *Talanta* 232.
- Yon, T., Sibat, M., Robert, E., Lhaute, K., Holland, W.C., Litaker, R.W., Bertrand, S., Hess, P., Réveillon, D., 2021b. Sulfo-Gambierones, two new analogs of Gambierone produced by *Gambierdiscus excentricus*. *Mar. Drug.* 19 (12).
- Yoshimatsu, T., Tie, C., Yamaguchi, H., Funaki, H., Honma, C., Tanaka, K., Adachi, M., 2016. The effects of light intensity on the growth of Japanese *Gambierdiscus* spp. (Dinophyceae). *Harmful. Algae.* 60, 107–115.